Laser-induced plasma applications

Prof. Walid Tawfik

National Institute of Laser Enhanced Sciences NILES, Department of Environmental applications,
Cairo University, Cairo, Egypt.

Walid_tawfik@niles.edu.eg

Walid_tawfik@Hotmail.com

01007869651

Laser Induced Plasma Spectroscopy (LIPS) as Elemental Analytical Technique

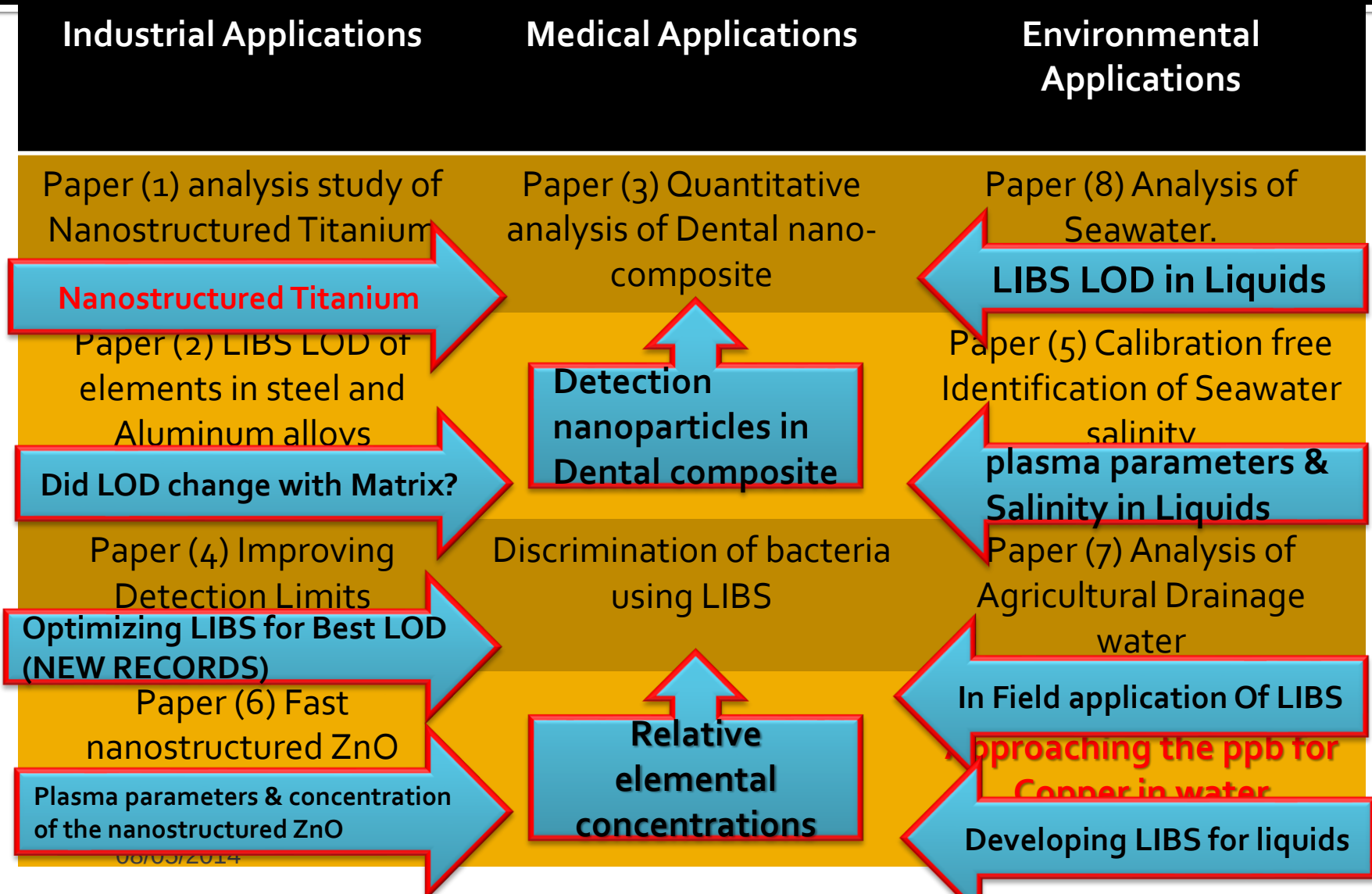

Industrial applications Papers

Samples of interest

1- Aluminum Alloys (very important 80%)

2- Steel Alloys (20 %)

Paper (1)

Comparative study of two new commercial Echelle spectrometers equipped with intensified CCD for analysis of laser-induced breakdown spectroscopy

Abstract

The purpose of this paper is to provide the reader with comparative information about two new commercial Echelle spectrometers equipped with intensified CCD ICCD detectors for laser-induced breakdown spectroscopy analysis. We carried out a performance comparison between two commercial ICCD Echelle spectrometers ESA 3000 LLA Instruments GmbH, Berlin-Adlershof, Germany and a Mechelle 7500 Multichannel Instruments, Stockholm, Sweden for the determination of the concentrations of Si, Mg, Cu, Mn and Be in the same Al alloy samples adopting the same experimental conditions. The results show that both systems, despite their differences in terms of resolution, have similar performance in terms of sensitivity and precision of measurements for these elements in an Al alloy matrix at least for the range of wavelength 280–400 nm studied in this work.

INTRODUCTION
How Echelle spectrometers works?

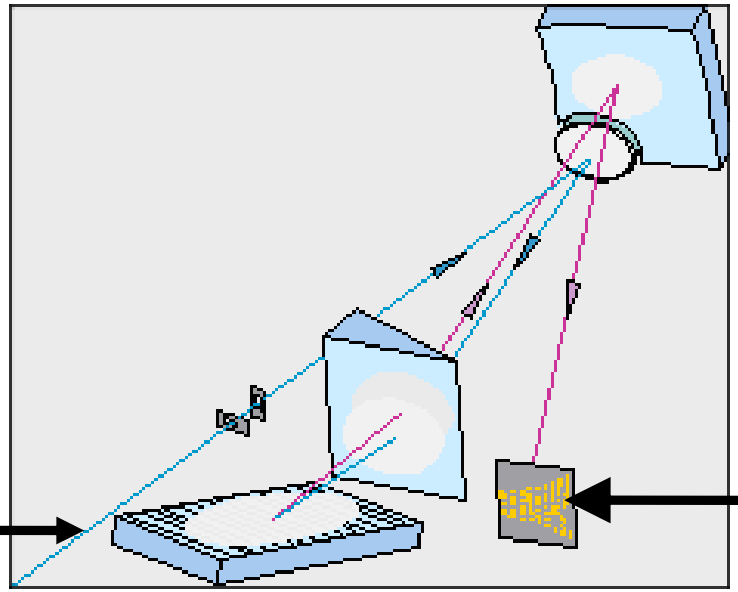

An Echelle grating, which is positioned under a flat angle of incidence, produces up to 100 overlapping diffraction orders. An additional quartz prism in front of the grating separates the overlapping orders by splitting them vertically to the direction of the spectrum. In that way the compact Echelle spectrograph covers a total spectrum length of over one meter on a one square inch focal plane. The optical parameters of the entire setup fit the relevant spectral range to the sensitive range of the camera of 25 mm x 25 mm. The linear dispersion is fitted to the pixel size of the camera

The Detector : Intensified coupled charged devices (ICCD)

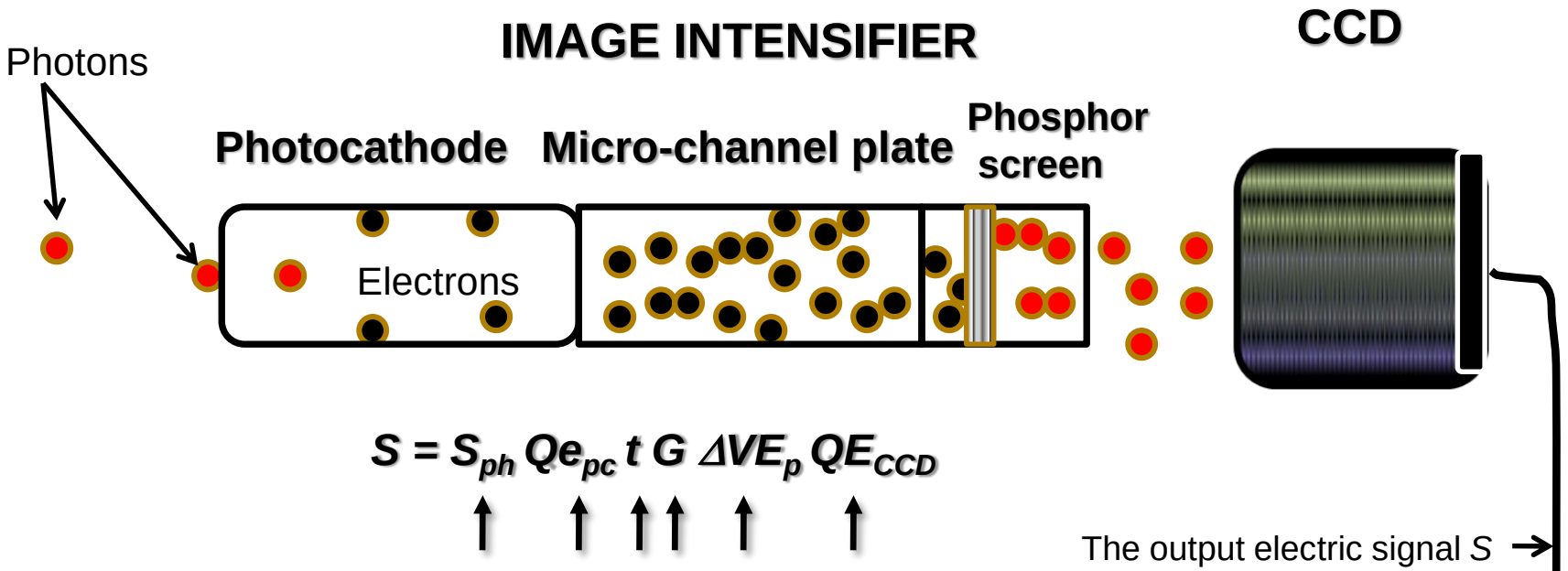

$$S = S_{ph}\, Qe_{pc}\, t\, G\, \Delta V E_p\, QE_{CCD}$$

The output electric signal *S*

The response of these parameters is not equal throughout the spectral range

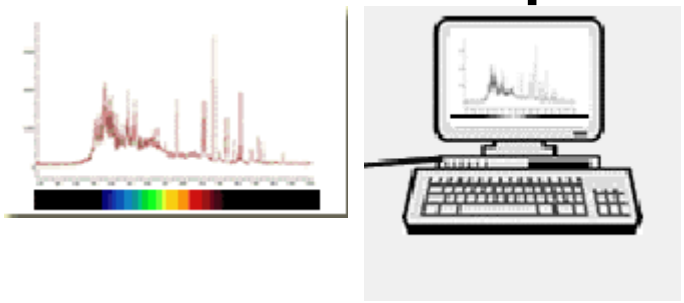

S_{ph} :the average photon flux incident on the photocathode
Qe_{pc}: the average quantum efficiency value across the photocathode in units of photoelectrons per photon.
t : the signal integration time
G : the current gain amplification of the MCP
V : the difference between the output and phosphor voltage
E_p: the average phosphor efficiency for converting electrons to photons
QE_{CCD}: the average conversion efficiency of phosphor photon signal to CCD electrons.

Steps

- 1- Applying both spectrometers in two completely identical LIBS setups for analysis of Aluminum Alloys.
- 2- Compare the obtained LIBS spectra for qualitative analysis.
- 3- Applying the internal standardization method to get linear calibration curves.
- 4- compare the obtained calibration curves.
- 5- compare the obtained LOD values for the two systems.

The two LIBS setups A,B used for analysis of Aluminum alloy samples

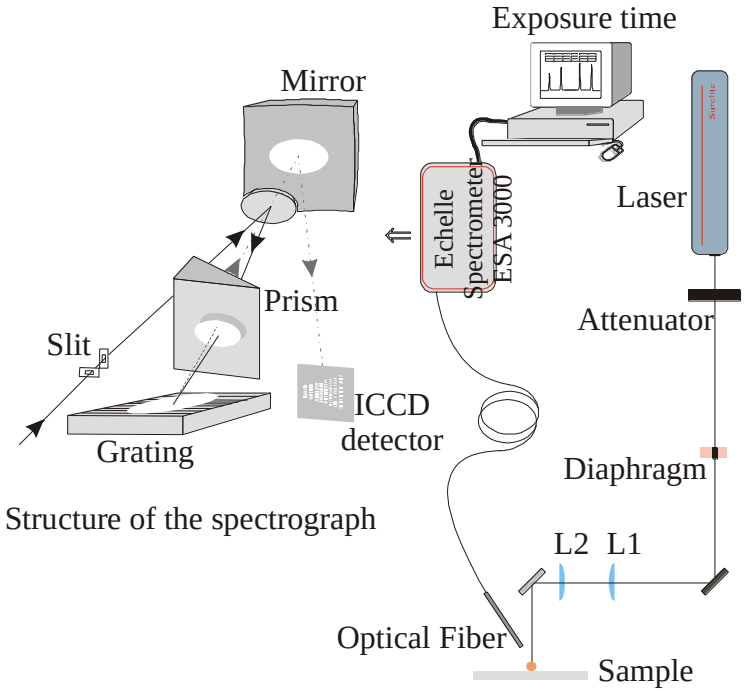

Experimental setup at NRC with system A

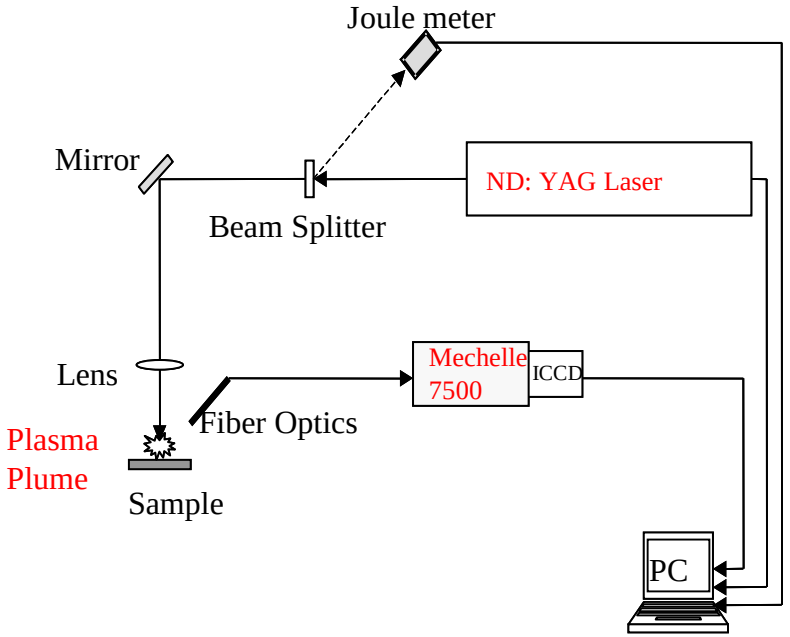

Experimental setup at NILES with System B

System A

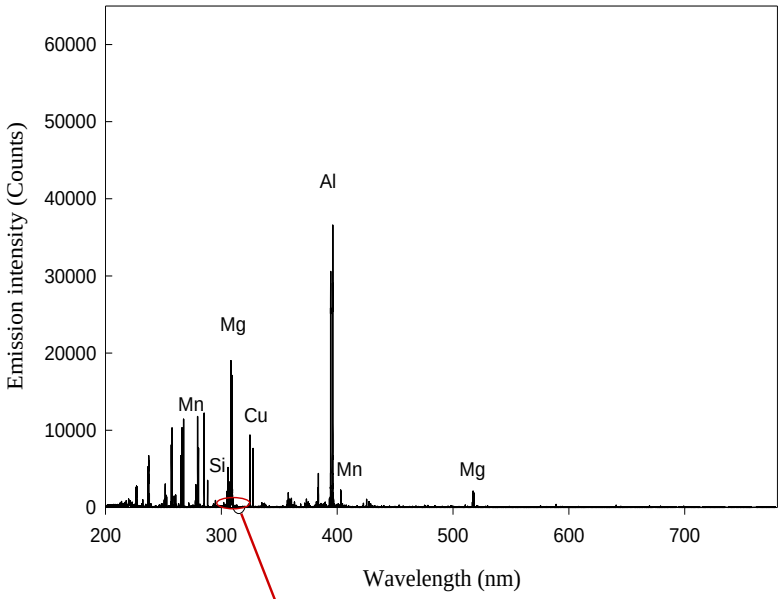

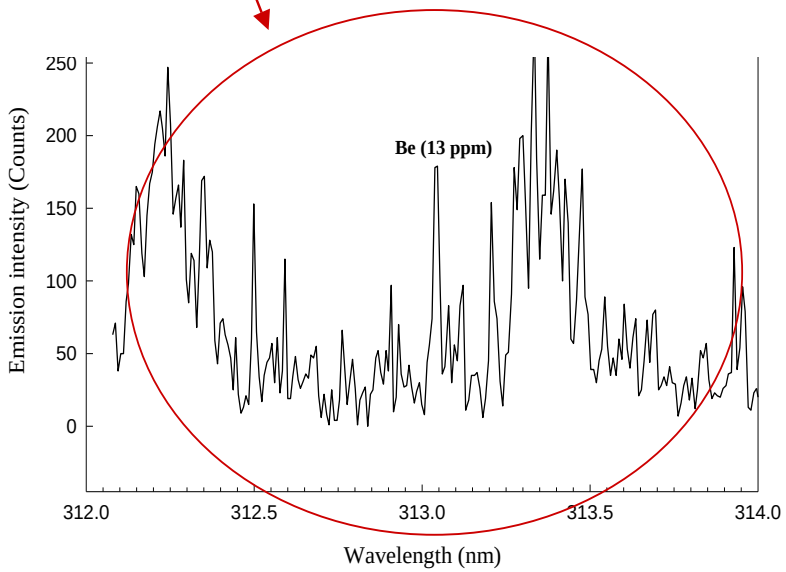

System B

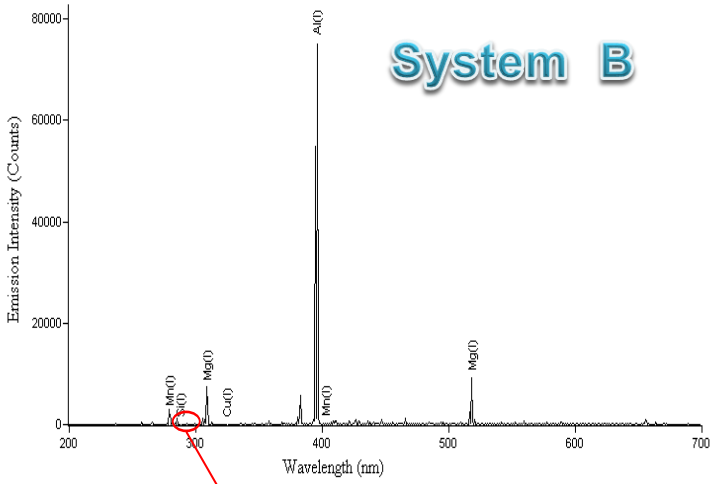

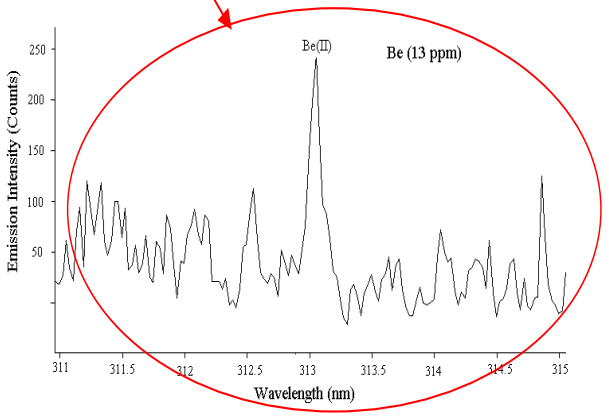

Recommended Conditions for the two LIBS systems

1- Laser Energy 60 mj

2- Laser wavelength 1064 nm

3- Laser pulse duration 10 ns

4- For system A : Delay time 3 μs and gate time 1 μs

5- For system B : Delay time 1.5 μs and gate time 3 μs

Recommended spectral Bandwidth for the two systems

(280 - 400 nm)

Manganese calibration curve in Al Alloys

Internal

Standardization

non-normalized

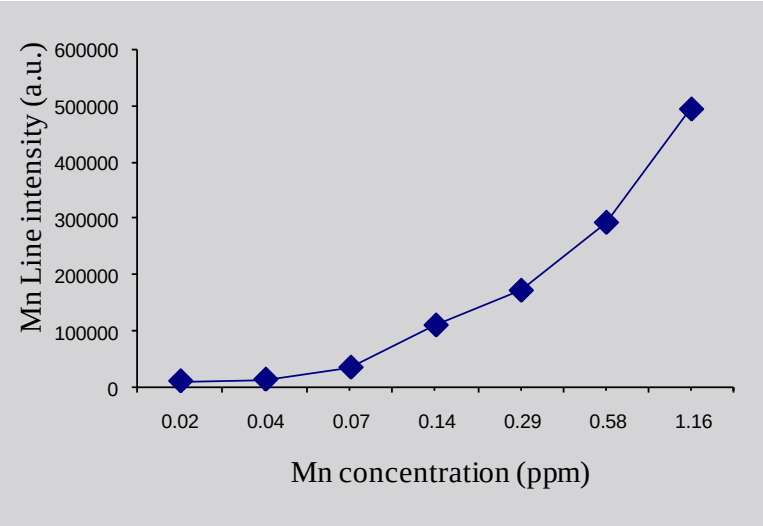

normalized

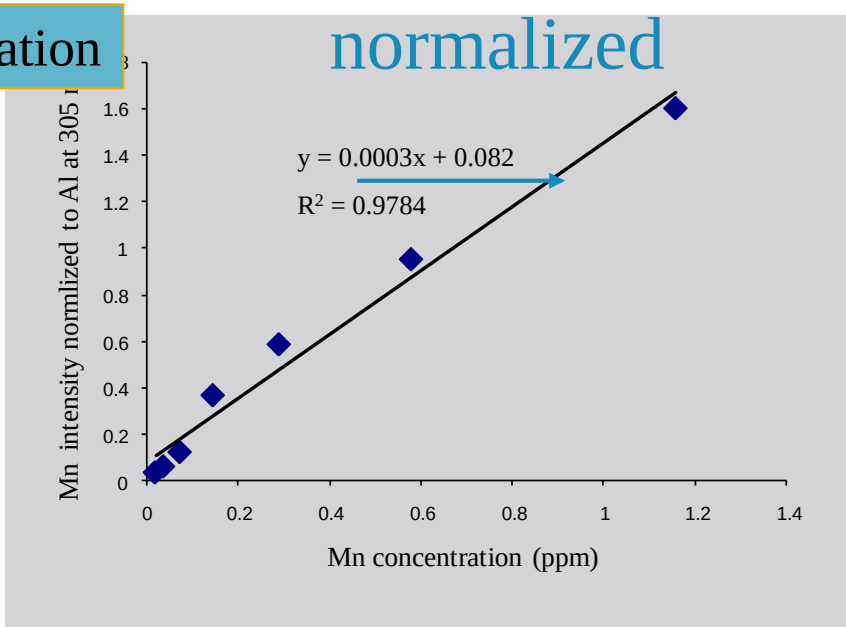

The manganese calibration curves for the two systems

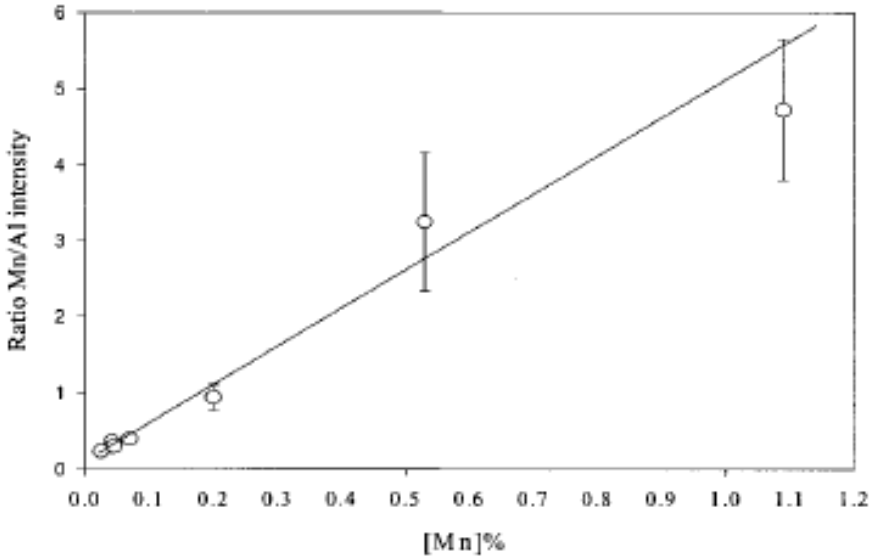

Fig. 5. Calibration curve of Mn obtained by System A.

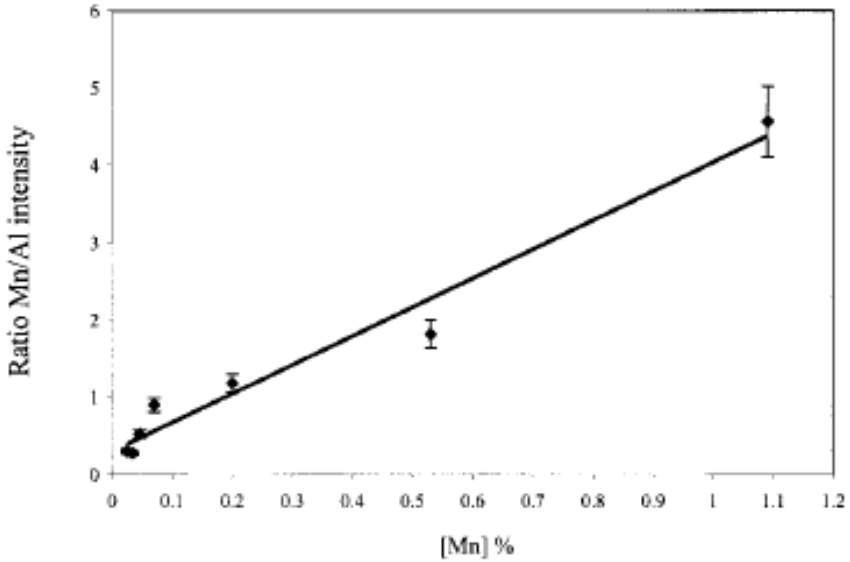

Fig. 6. Calibration curve of Mn obtained by System B.

The limits of Detection of the two systems observed for some elements in Aluminum alloy samples

Table 1. Limit of Detection for Various Elements in the Same Aluminum Alloys Obtained by Systems A and B

Element	Wavelength of the Spectral Line Used (nm)	LOD	
		System A LLA Echelle/ICCD (ppm)	System B Mechelle/ICCD (ppm)
Be	313.0	1.6	0.4
Mg	285.21	9	5.5
Si	288.16	90	136.6
Mn	403.0	65	18
Cu	324.75	33	30.4

Conclusion

In summary we have carried out a comparative study between two commercial Echelle spectrometers equipped with ICCD UV enhanced detectors in terms of spectrochemical analysis by LIBS of five trace elements in aluminum alloy samples. The two systems are exploited in two typical LIBS setups running under nearly the same experimental conditions. The results showed that both systems have similar limit of detection of the five investigated elements when spectral lines in the UV- range **(280-400 nm)** are used in the analysis. For industrial applications, both systems could be used to detect trace elements at ppm concentrations in metallic alloys.

Paper (2)
LIBS limit of detection and plasma parameters of some elements in two different metallic matrices

In the present work we aim to study the effect of the matrix on the LIBS limit of detection (LOD) of four elements (Mg, Si, Mn, and Cu) in two different matrices, aluminum and steel standard alloys under same experimental conditions. A detailed investigation of the plasma parameters of the two alloys is presented and correlated to the matrix effect too.

Elements of Interest

- Silicon
- Copper
- Manganese
- Magnesium

Steps

1- Applying the same LIBS setup for analysis of both Aluminum and steel Alloys.

2-Optimize the time delay for both ionic and atomic lines.

3-Compare the obtained LIBS spectra for qualitative analysis.

4- Compare the obtained calibration curves.

5- Compare the Boltzmann plots for both Aluminum and steel Alloys.

6- Determine the plasma temporal behavior for both Aluminum and steel Alloys.

7- Compare the obtained LOD values for the two alloys.

Optimization curve for the delay time using both ionic and neutral lines in order to obtain best detection limit.

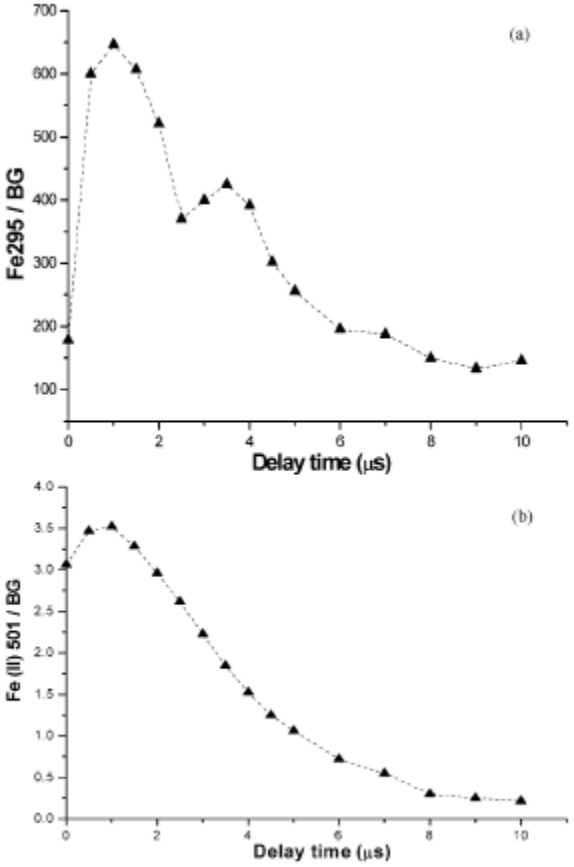

Fig. 1 (a) Delay time optimization of neutral lines. (b) Delay time optimization of ionic lines.

Typical LIBS spectrum for aluminum and steel alloy.

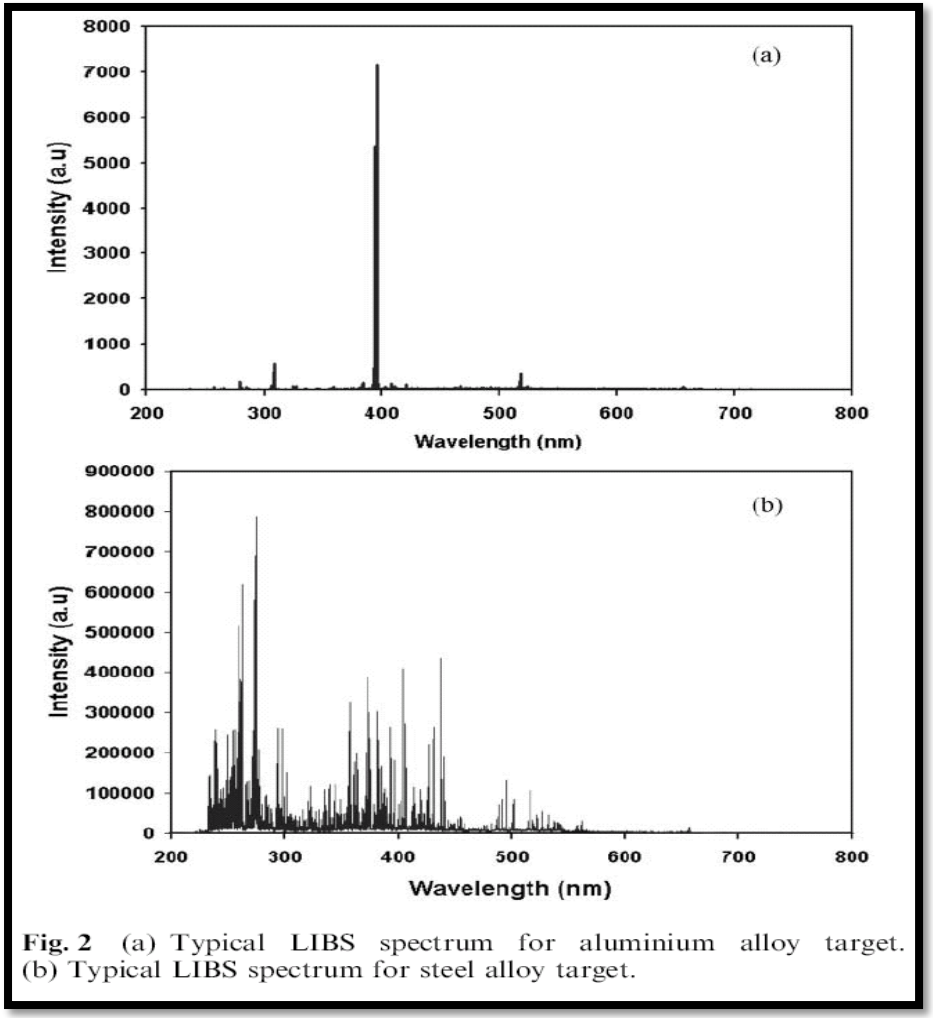

Fig. 2 (a) Typical LIBS spectrum for aluminium alloy target. (b) Typical LIBS spectrum for steel alloy target.

Calibration curves of Silicon in aluminum and steel alloys

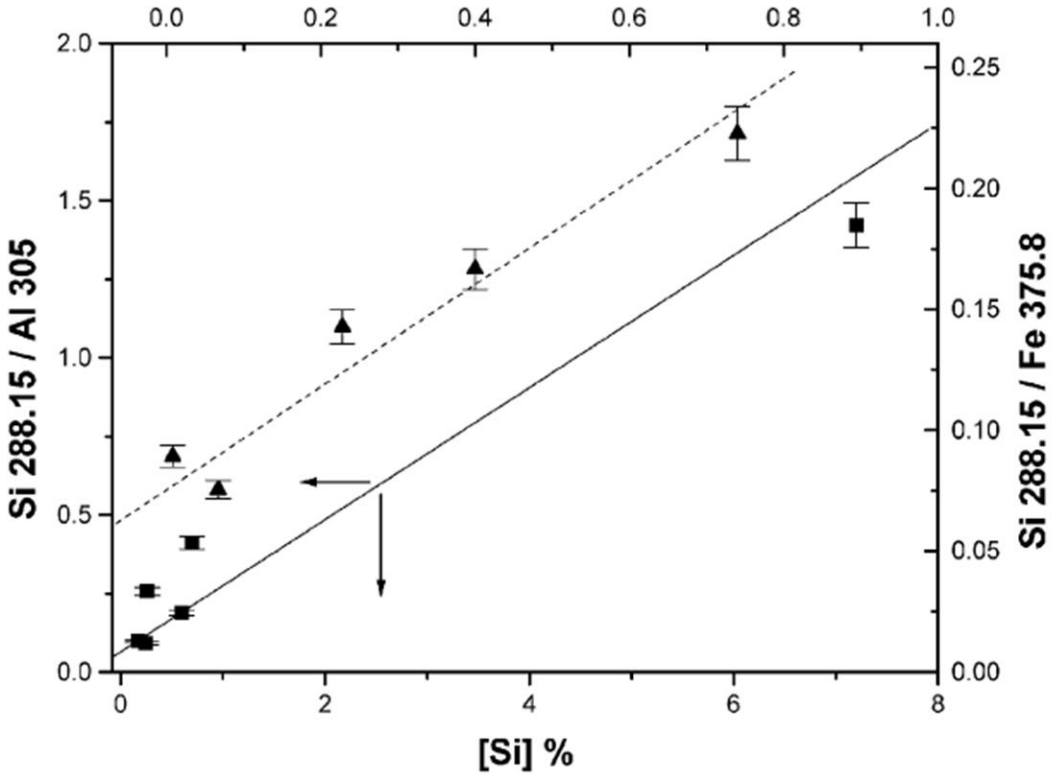

Fig. 4 Calibration curves of Si in aluminium alloy (squares) and in steel alloy (triangles).

Calibration curves of Manganese in aluminum and steel alloys

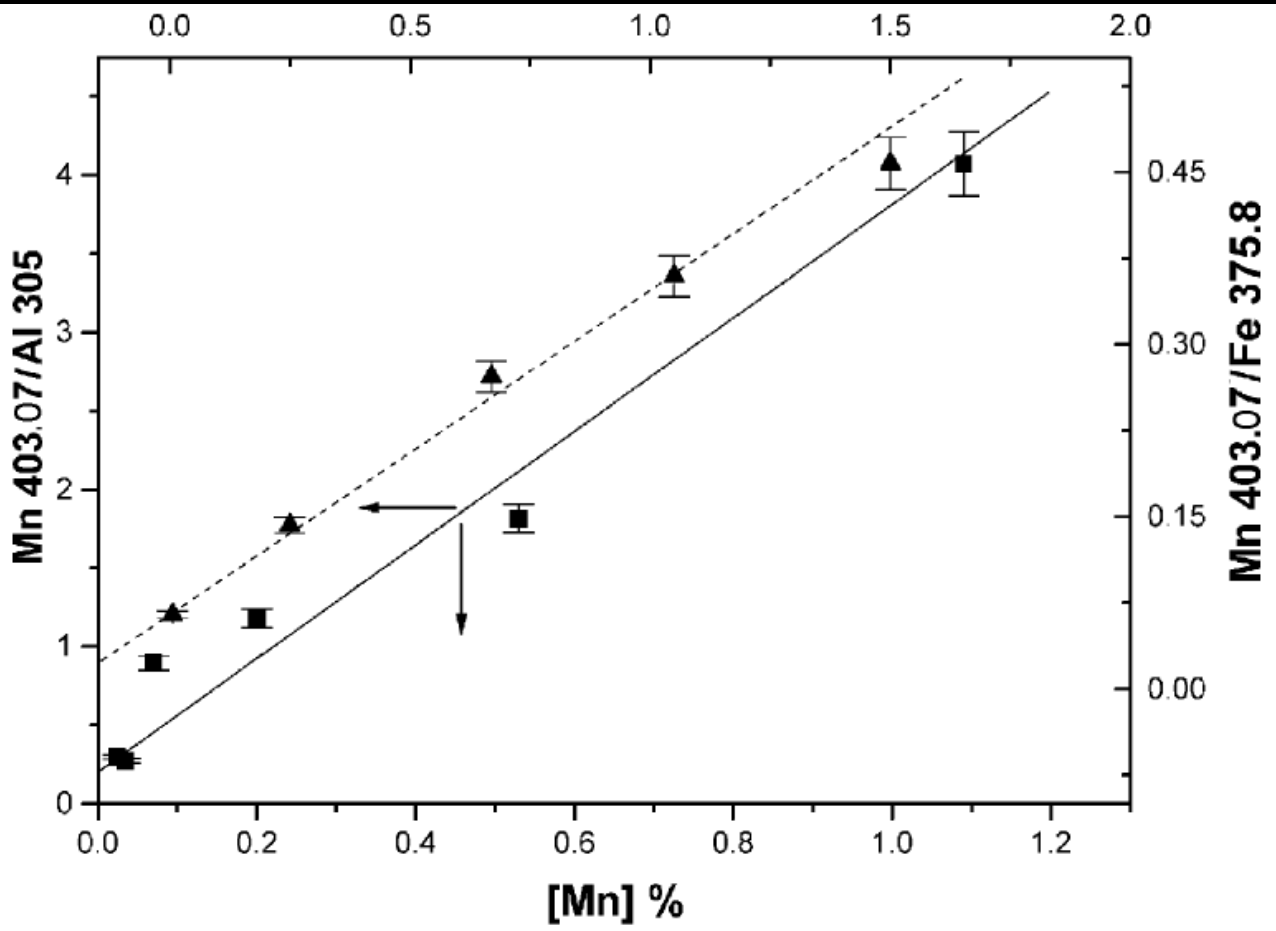

Fig. 5 Calibration curves of Mn in aluminium alloy (squares) and in steel alloy (triangles).

Calibration curves of copper in aluminum and steel alloys

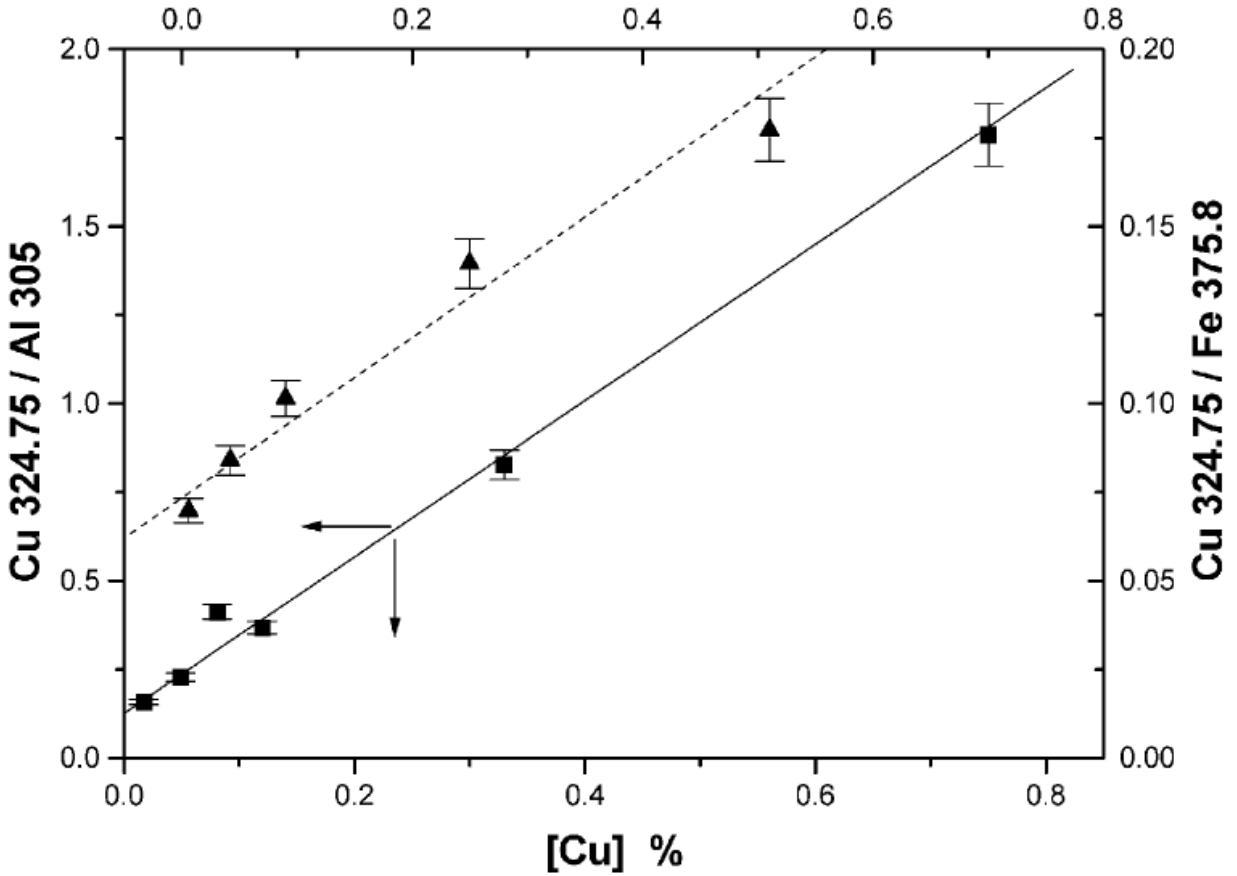

Fig. 6 Calibration curves of Cu in aluminium alloy (squares) and in steel alloy (triangles).

Boltzmann plots for aluminum and steel alloys.

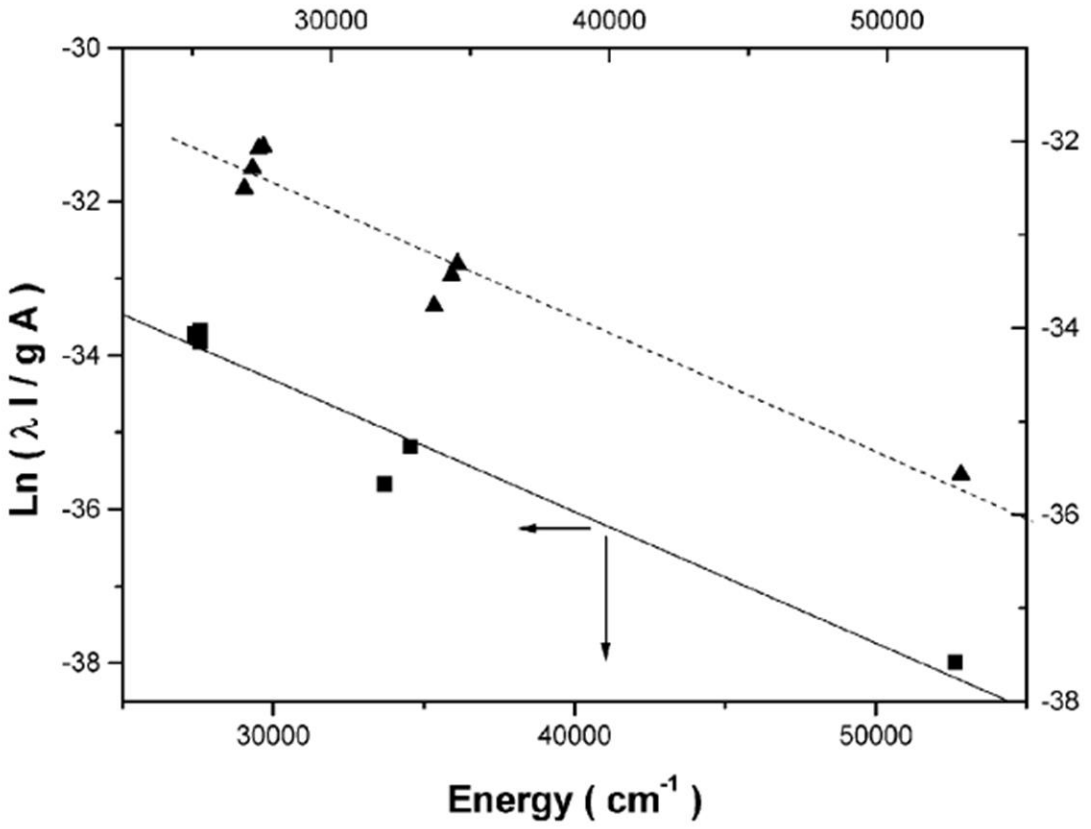

Fig. 7 Typical Boltzmann plots for aluminium alloy (squares) and for steel alloy (triangles).

Temporal behavior of plasma temperature of aluminum and steel alloys

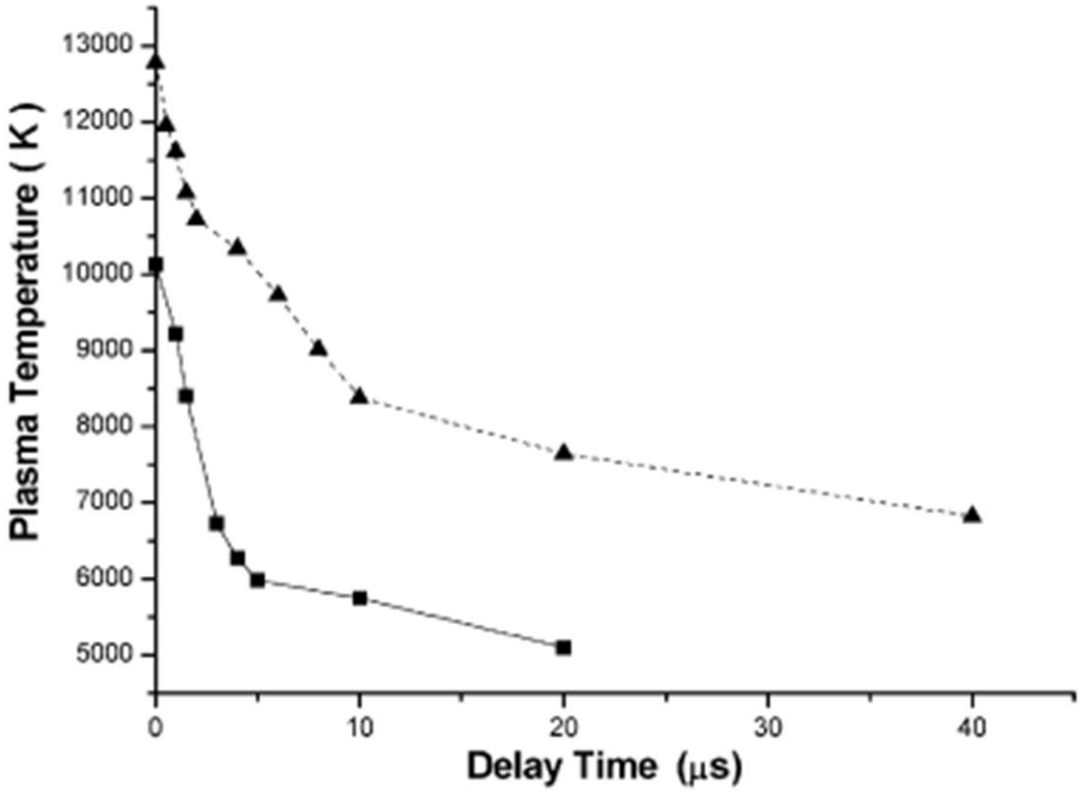

Fig. 8 Temporal behavior of plasma temperature of aluminium alloy (squares) and for steel alloy (triangles).

Temporal behavior of plasma density of aluminum and steel alloys

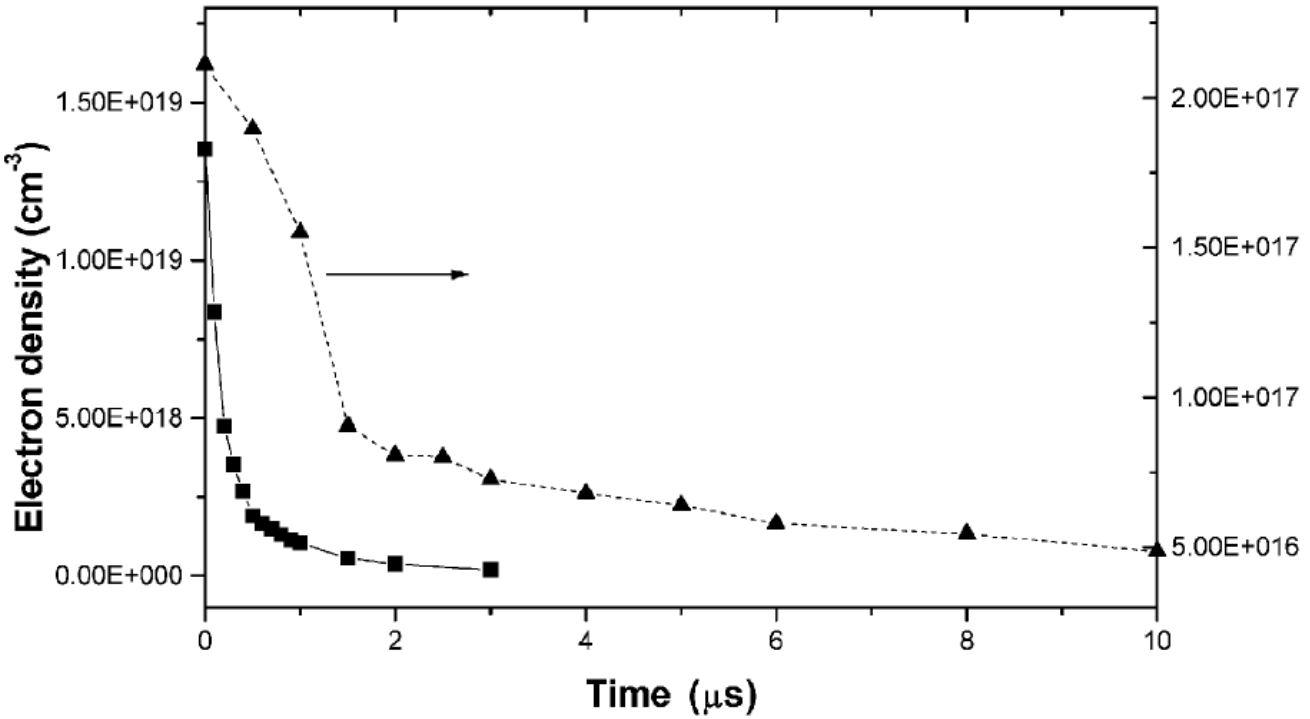

Fig. 9 Temporal behavior of plasma density for aluminium alloy (squares), and for steel alloy (triangles).

Comparison between Limit of detection (LOD) for aluminum and steel alloys.

Table 3 Limit of detection (LOD), relative standard deviation (RSD%), and correlation coefficient (R^2) values for the elements under study in aluminium alloy

Wavelength	LOD (ppm)	RSD%	R^2
Mg (285 nm)	28.16	3.1	0.99
Si (288 nm)	283.9	9.12	0.98
Mn (403 nm)	15.28	3.17	0.98
Cu (324 nm)	23.8	5.05	0.99

Table 4 Limit of detection (LOD), relative standard deviation (RSD%), and correlation coefficient (R^2) values for the elements under study in steel alloy

Wavelength	LOD (ppm)	RSD%	R^2
Mg (285 nm)	76.78	4.12	0.56
Si (288 nm)	6.64	1.46	0.97
Mn (403 nm)	4.99	3.41	0.99
Cu (324 nm)	6.31	6.31	0.98

Why?

Mg has much lower LOD in the aluminum alloy matrix than in steel alloy matrix.

Table 5 Physical constants of different elements in the investigated samples

Element	Atomic number	Atomic weight/u	Boiling point/K	Melting point/K	Specific heat/J gm^{-1} K^{-1}
Mg	12	24.305	1363	922	1.02
Al	13	26.98	2740	933.52	0.9
Si	14	28.08	2628	1683	0.71
Mn	25	54.93	2235	1517	0.48
Fe	26	55.84	3023	1809	0.444
Cu	29	63.54	2836	1356.6	0.38

Affecting the energy transfer between the elements within each matrix

Conclusion

1- The present investigations show that, the differences in the LIBS LOD of the same elements in different matrices can be correlated to the compatibility of the physical properties of the elements existing in the same matrix. So that, the target physical properties play an important role in the obtained values of the LIBS LOD.

2- The temporal behavior of the plasma temperature and density showed that the plasma of the aluminum alloy cooling down faster than the plasma of the steel alloy. This indicates that the recombination processes in Al alloys is much faster than the steel alloys.

3- The obtained results indicate that it is possible to apply LIBS in the on-line industrial process control

Paper (4)

Improved LIBS Limit of Detection of Fe, Mg, Be, Si, Mn and Cu in Aluminum Alloy Samples Using a Portable Echelle Spectrometer with ICCD Camera

Abstract

In the present work, Laser-induced breakdown spectroscopy LIBS has been applied to perform elemental analysis of five trace elements simultaneously in aluminum alloy targets. The plasma is generated by focusing a pulsed Nd: YAG laser on the target in air at atmospheric pressure. The produced plasma emissions were detected using a time-resolved high resolution Echelle spectrometer that provides a constant spectral resolution (CSR) of 7500 corresponding to 4 pixels FWHM over a wavelength range 200 – 1000 nm displayable in a single spectrum. LIBS limit of detection (LOD) is affected by many experimental parameters such as; interferences, self-absorption, spectral overlap and matrix effect. We aimed to improve the LIBS LOD by optimizing these experimental parameters as possible. It is found that, applying 10^{10} W/cm^2 laser irradiance at the sample surface, recording plasma emission spectra at 2.5 μs delay time and 1.5 μs gate time, wavelength calibrating the spectrometer using a mercury lamp source, controlling the laboratory temperature to be approximately fixed, avoiding self-absorption and spectral overlap by selecting proper wavelengths for the determined elements are the key conditions for observing improvements in LOD values. In doing so, the calibration curves for beryllium, magnesium, silicon, manganese and copper as minor elements were achieved with linear regression coefficients between 98–99% on average in aluminum alloy samples. New LOD values were achieved for these elements in the ppm range with high precision (RSD 3 – 8 %). From the application view point, improving LIBS LOD is very important for the on-line industrial process control which may enables LIBS to be used in following up multi-elements for the correct alloying in metals in future.

The key conditions for observing improvements in LOD values

1- Increasing the laser irradiance from 10^8 W/cm^2 to 10^{10} W/cm^2.
2- Optimizing the delay time and the gate time to 2.5 μs delay time and 1.5 μs gate width.

reducing the background signal, **increasing the SNR** of the ppm trace elements and increasing the spectral resolution. The observed resolution of 0.045 nm for beryllium line at 313.03 nm is about five times higher than observed before (0.2 nm).

3- we found that the ICCD camera depends on thermoelectric cooling to maintain its temperature exactly -15 C° . So any small variation the laboratory temperature affecting the camera and cause the spectrum shifts approximately 5-25 pixels. To avoid this problem, the laboratory temperature is controlled to be approximately fixed and the spectrometer is wavelength calibrated from time to time using a mercury lamp source (Hg lines at 253.65, 435.83, 546.07 nm).

The key conditions for observing improvements in LOD values cont.

4- New Al alloy samples were selected, so that the trace elements concentrations were about ten times lower than samples used in previous work.

5- Laser shot-to-shot variation causes differences in the plasma properties, therefore affects the magnitude of the element signal, and hence degrades the LIBS precision. To improve LIBS precision, spectra from several laser shots have to be averaged in order to reduce statistical error due to laser shot-to-shot fluctuation. Moreover, we found that enhancement of the data reproducibility can be achieved by accumulation of consecutive measured spectra. We reproduced the measurements at five locations on the sample surface in order to avoid problems linked to sample heterogeneity. Twenty shots were fired at each location and saved in separated files and the average was computed and saved to serve as the library spectrum.

The key conditions for observing improvements in LOD values cont.

6- The performed optimization in case of the minor elements in the aluminum alloy revealed that the best internal standard is the Al atomic line at 305 nm.

7- To avoid self-absorption and spectral line interference,

1- Avoiding the possibility of self-absorption in the case of lines ending to a heavily populated level, such as resonance lines. So that lines like **Al (394.5 nm), Al (396.26nm),** Al (308.30 nm), Al (309.36 nm), Si (251.50 nm) were avoided.

2-Avoiding interference between spectral lines for different species. So that, interfering lines like **Fe (285.3 nm) and Mg (285.29nm),** and similar lines were avoided.

Selecting proper wavelengths for each element from broad Band LIBS Spectrum

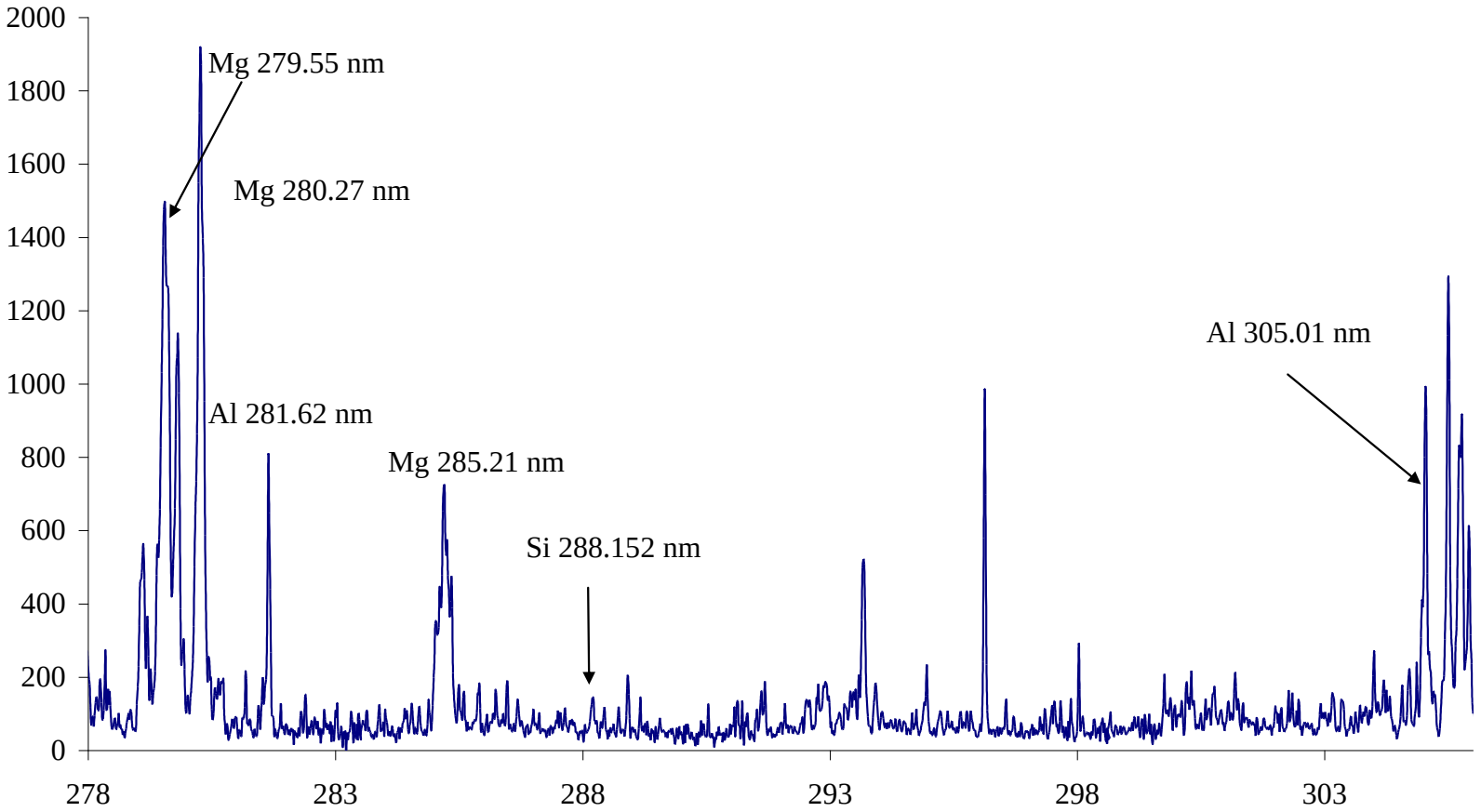

Increasing the resolution five times

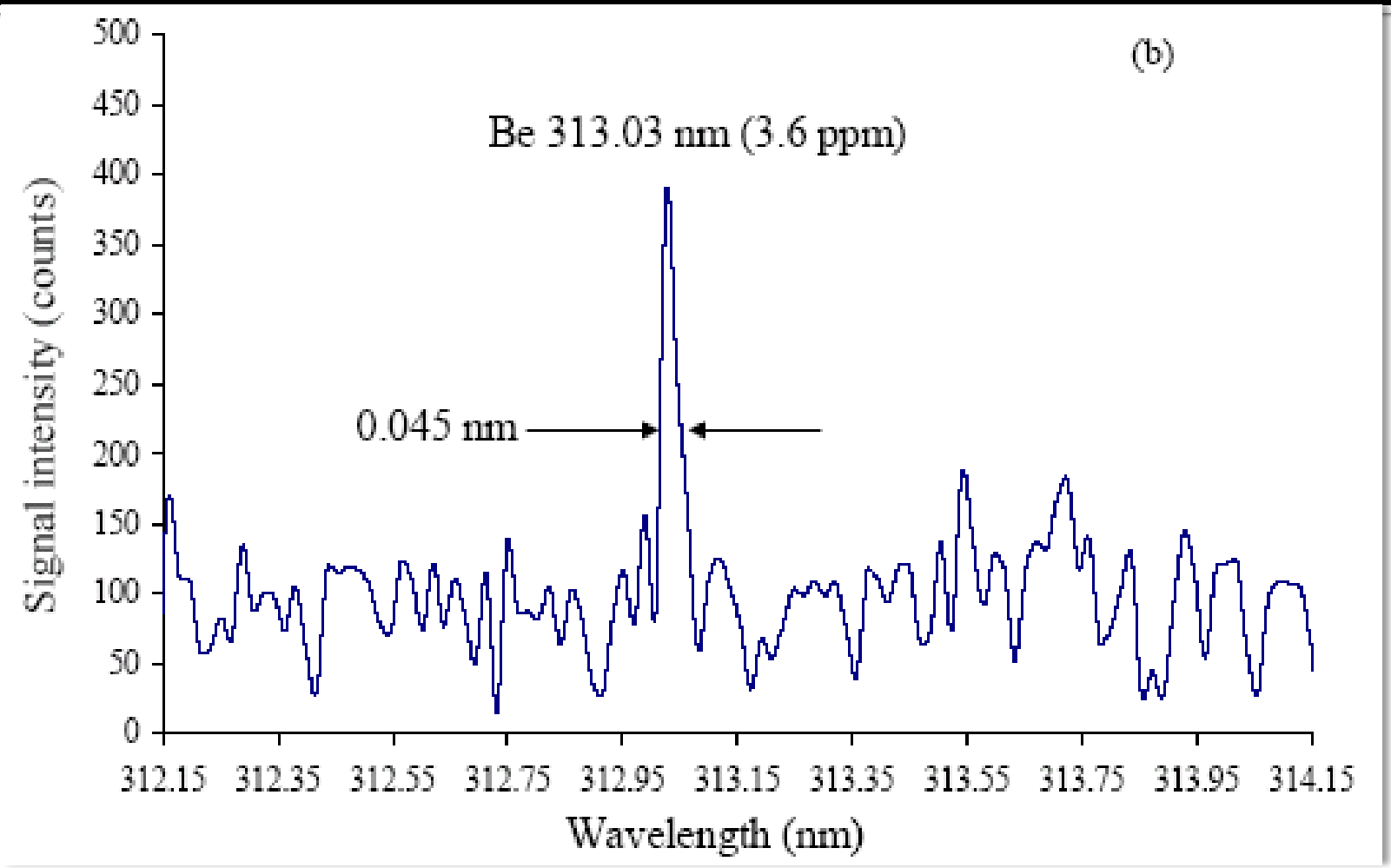

Improved calibration curves for Fe, Cu, Mg, Mn, Be and Si in aluminum alloy samples

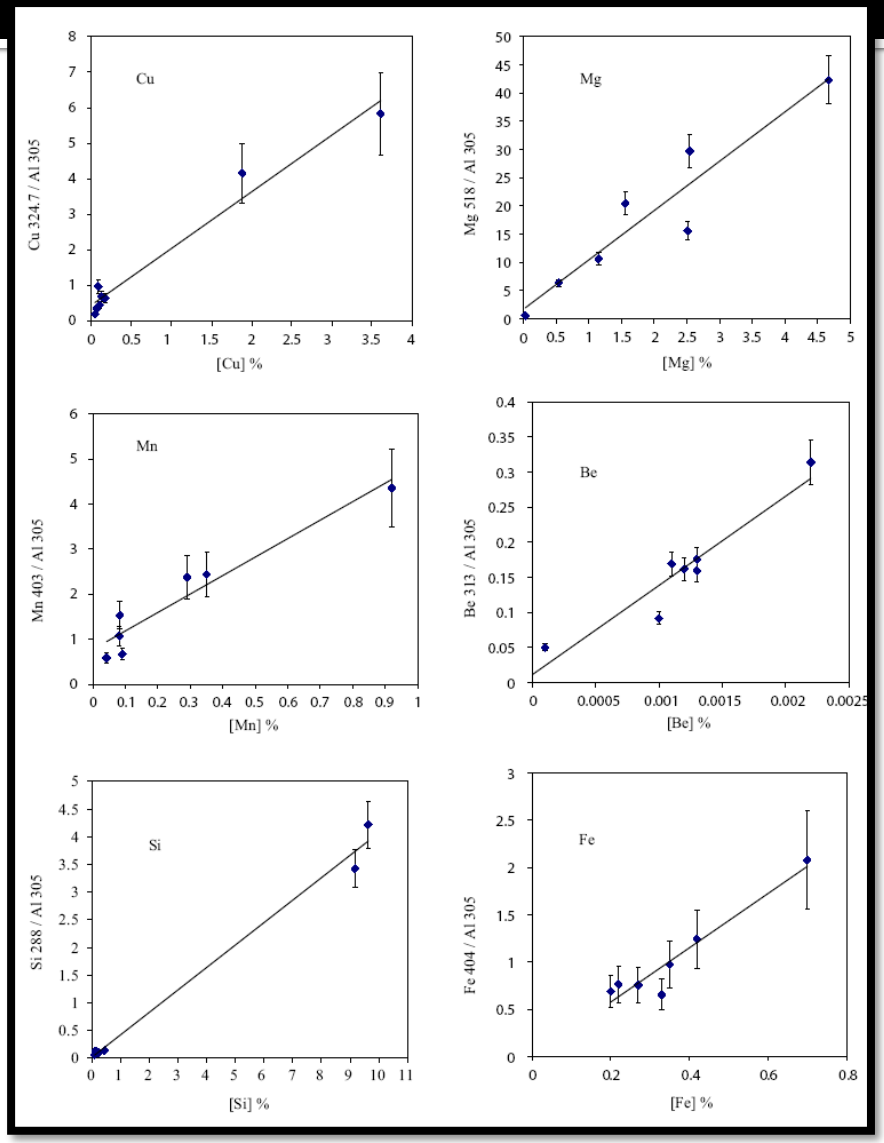

New Records for the Limit of detection (LOD) values

Element	wavelength of the spectral line used (nm)	**LOD values (ppm) This work**	LOD values (ppm) Previous work [7]	RSD%	R^2	Calibration equation
Be	313.05	**0.22**	0.4	8.22%	0.9015	y = 127.05x + 0.0113
Fe	404.58	**9.71**	84.5	8.23%	0.9193	y = 2.8691x + 0.0011
Mg	518.36	**3.19**	5.5	3.35%	0.8965	y = 8.7427x + 1.6886
Si	288.152	**68.74**	136	8.74%	0.9908	y = 0.4051x + 0.0207
Mn	403	**6.81**	18	4.94%	0.9252	y = 4.0952x + 0.7778
Cu	324.75	**17.49**	30.4	5.59%	0.9691	y = 1.5924x + 0.4500

(RSD %) relative standard deviation, (R^2) correlation coefficient values.

Conclusion

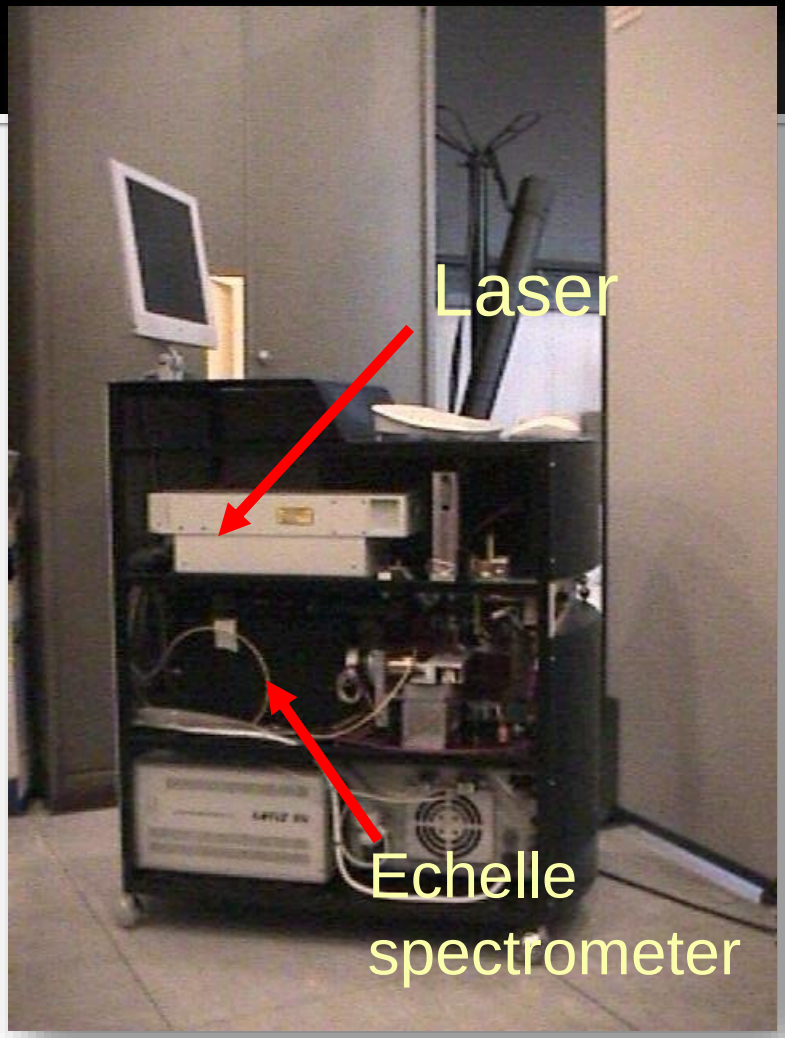

1-New records

The obtained results showed that by optimizing the experimental parameters and carefully selecting appropriate wavelength for each trace element, the detection limits for Fe, Mg, Be, Si, Mn and Cu are great better than the previously published values.

2- Proposed Portable LIBS

The proposed LIBS setup is compact and could be transported. In future, this system could be arranged in one cabinet with dimensions 80 x 80 x 100 cm since the Mechelle spectrometer including the ICCD camera is 30 cm length, 14 cm width and 17 cm height and the Nd: YAG laser (surelite I) is about 60 cm length, 15 cm width and 15 cm height).

3- Application

All of these facilitate LIBS to be used for in-situ real time industrial process control following up multi-elements for the correct alloying in metals and in pharmaceuticals.

Paper (6)
Fast LIBS Identification of Aluminum Alloys

Abstract

LIBS has been applied to analysis aluminum alloy targets. The plasma is generated by focusing a 300 mJ pulsed Nd: YAG laser on the target in air at atmospheric pressure. Such plasma emission spectrum was collected using a one-meter length wide band fused-silica optical fiber connected to a portable Echelle spectrometer with intensified CCD camera. Spectroscopic analysis of plasma evolution of laser produced plasmas has been characterized in terms of their spectra, electron density and electron temperature assuming the LTE and optically thin plasma conditions. The LIBS spectrum was optimized for high S/N ratio especially for trace elements. The electron temperature and density were determined using the emission intensity and stark broadening, respectively, of selected aluminum spectral lines. The values of plasma parameters were found to change with the aluminum alloy matrix, i.e. they could be used as a fingerprint character to distinguish between different aluminum alloy matrices using only one major element (aluminum) without needing to analysis the rest of elements in the matrix. Moreover, It was found that the values of Te and Ne decrease with increasing the trace elements concentrations in the aluminum alloy samples. The obtained results indicate that it is possible to improve the exploitation of LIBS in the remote on-line industrial monitoring application, by following up only the values of Te and Ne for the aluminum in aluminum alloys using an optical fiber probe.

For industrial applications, We want to save time and efforts

For fast Identification of Alloys in industrial applications, We need no calibration curves

Find a dependency between

Plasma parameters ⟷ **Concentrations of the elements**

Steps

1- Applying all possible enhancement conditions to increase the SNR.

2- Determine the plasma temperature and density for different alloy matrices having the same elements but with different concentrations.

3- Study the relation between these plasma parameters and if they change with the concentrations of the elements.

Enhancement of S/N ratio by using 10^{10} W/cm^2 laser irradiance, 2.5 μs delay time and 1.5 μs gate delay

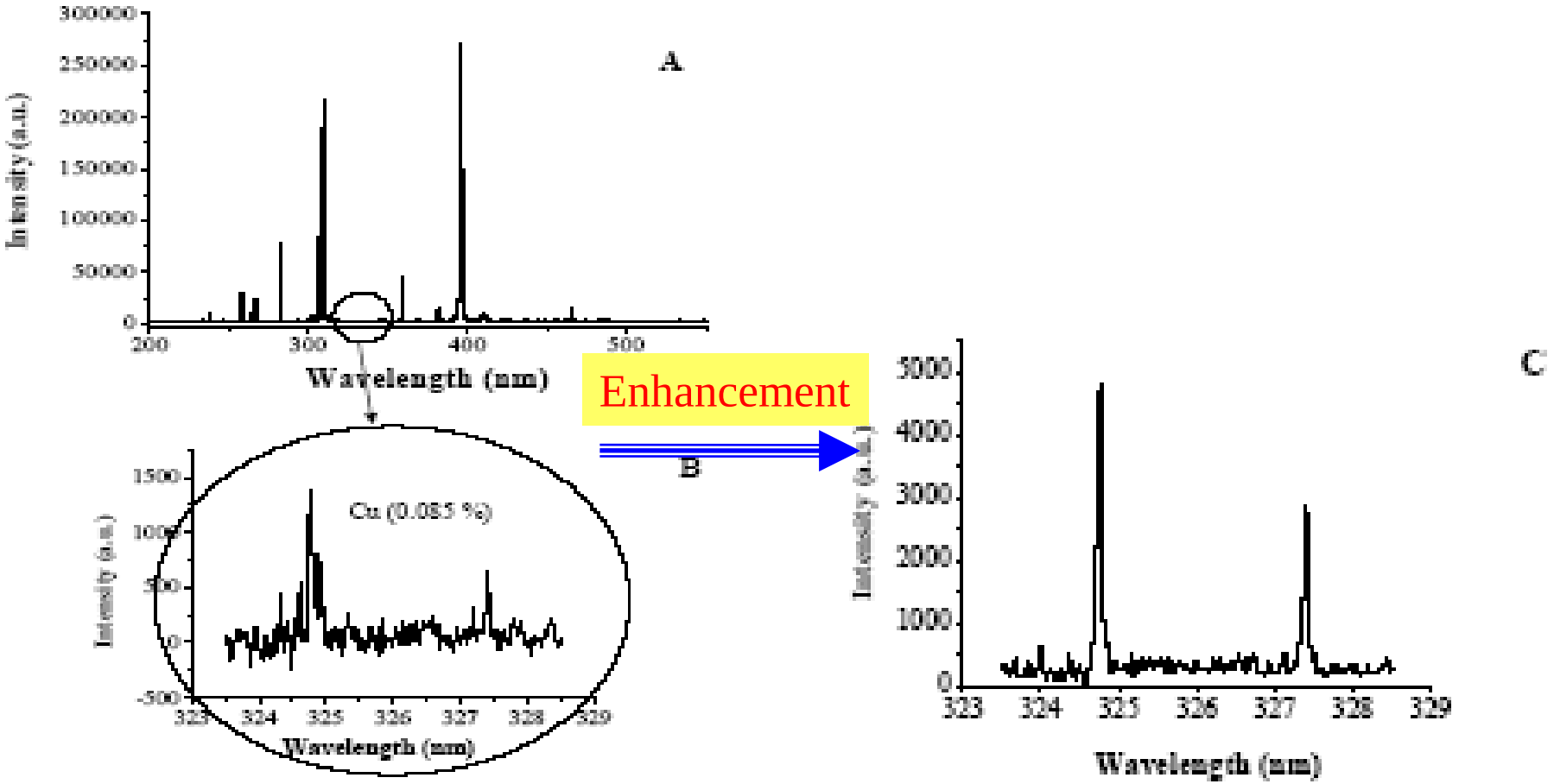

Four Boltzmann plots for aluminum in four different aluminum alloys. The slope of the plotted curves yields temperatures 13960 K, 12974 K, 11871 K, and 10841 K for the samples AL6063, AL 5754, AL 3104 and AL 4104, respectively.

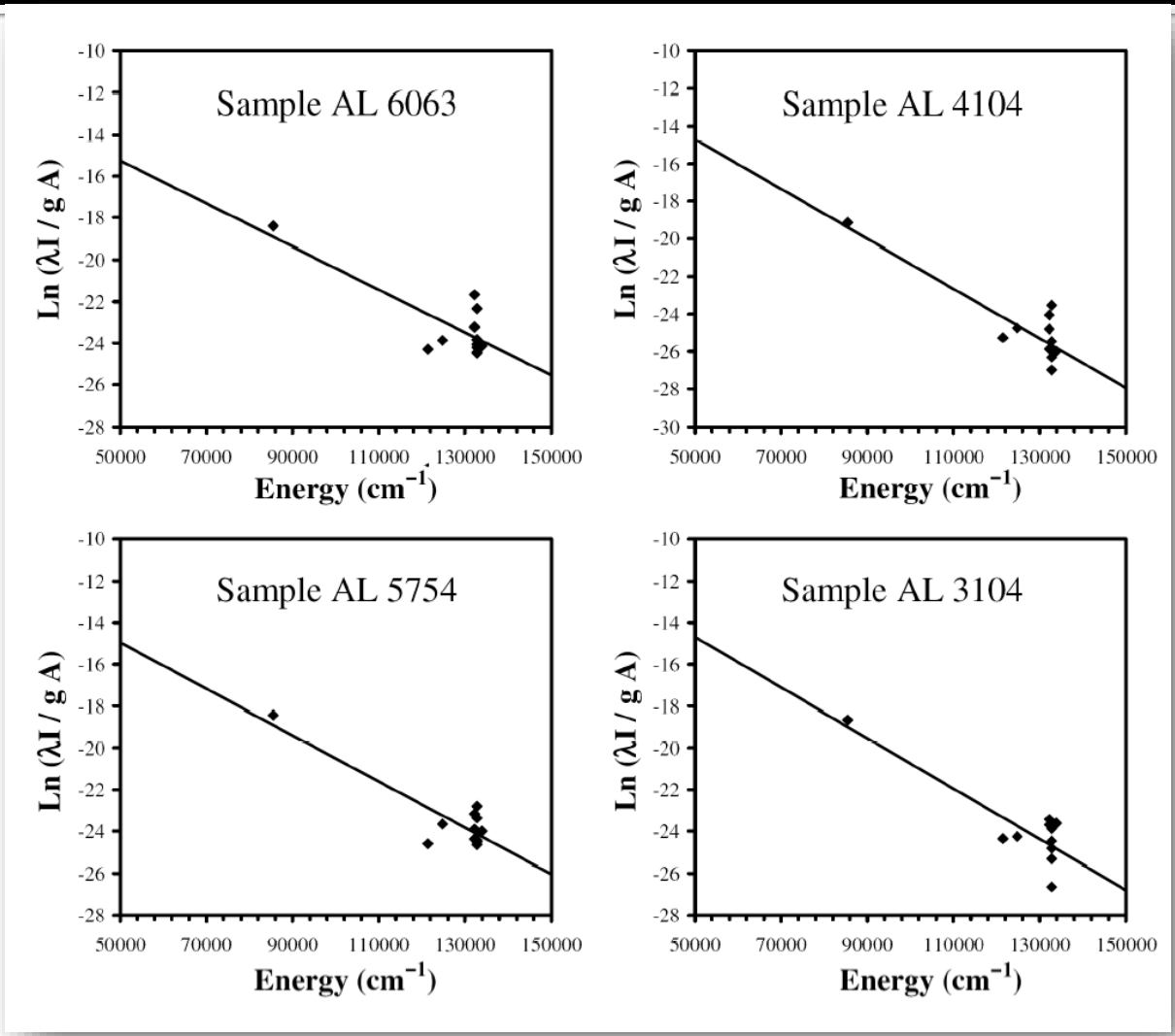

The 281.62 nm line with sufficient resolution to measure the full width at half-maximum ($\lambda_{1/2}$) at four different aluminum alloy samples to determine N_e

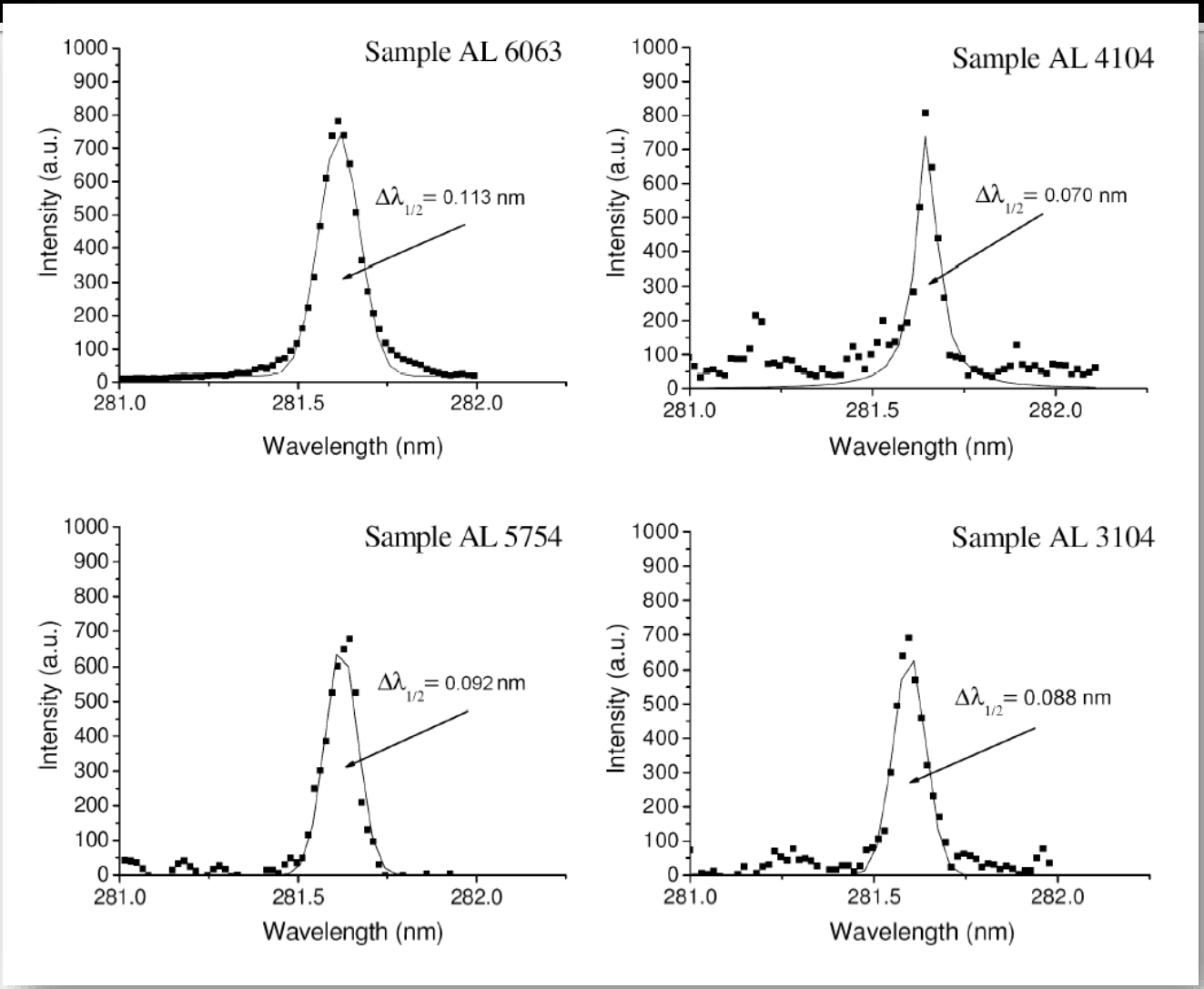

The plasma electron temperature Te and density Ne determined from aluminum spectral lines in the four standard aluminum alloy samples.

Why?

Plasma parameters			Sample AL 3104	Sample AL 4104
Electron Temperature (Kelvin)	13960	12974	11871	10841

1- Because increasing the "trace element" concentration comprises increasing portion of the laser-target interaction volume of that trace element and decreases the laser-target interaction volume of the major element (aluminum).

AL 6063	0.00030	0.54	0.43	0.2	0.085	0.0021	0.081	Balance

2- The ionization potential of Al, Ca, Be, Mg, Si, Mn, Fe, and Cu are (in eV) 5.98, 6.11, 9.32, 7.64, 8.15, 7.43, 7.87 and 7.72 respectively. This indicates that aluminum "the major element" species are easy to be ionized than the species of the seven trace elements which leads to higher electron density for aluminum alloy samples with low trace elements concentrations than for relatively high trace elements concentrations.

How the laser-target interaction volume changes with increasing the trace elements concentrations?

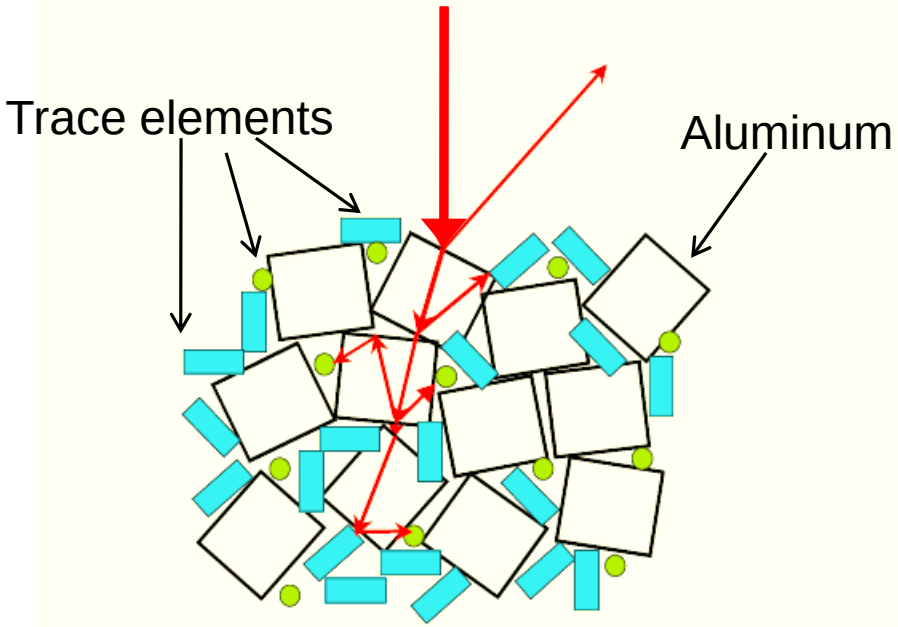

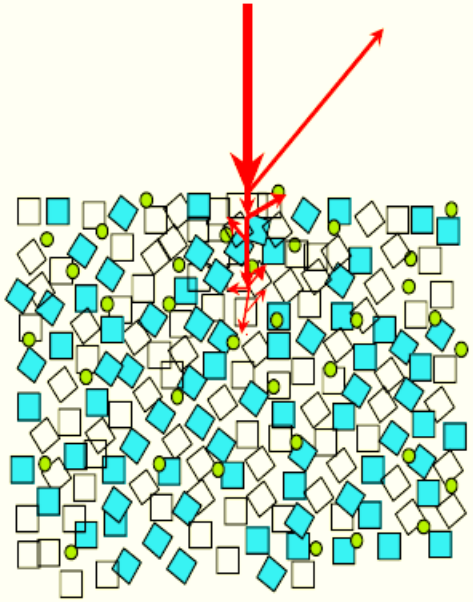

Low Trace elements concentration

High Trace elements concentration

Conclusion

- LIBS technique has been used to analysis different aluminum alloy samples. The LIBS spectrum was optimized for high S/N ratio especially for trace elements. The characteristic plasma parameters (Te , Ne) were determined using selected aluminum spectral lines. The values of these parameters were found to change with the aluminum alloy matrix, i.e. they could be used as a fingerprint character to distinguish between different aluminum alloy matrices using only one major element (aluminum) without needing to analysis the rest of elements in the matrix. Moreover, It was found that the values of Te and Ne decrease with increasing the trace elements concentrations in the aluminum alloy samples.

- For industrial applications, LIBS could be applied in the on-line industrial process that following up elemental concentration in aluminum alloys by only measuring Te and Ne for the aluminum using an optical fiber probe. This could be done by building a database containing the determined values of Te and Ne for a range of standard aluminum alloy matrices. Then the unknown aluminum alloy sample could be identified just by comparing its measured Te and Ne values with the previously stored values in our database.

Medical applications Paper

Paper (3)

Quantitative analysis of mercury in silver dental amalgam alloy using laser induced breakdown spectroscopy with a portable Echelle spectrometer

Abstract

In the present work, the proposed LIBS setup has been applied to perform elemental analysis of mercury in platinum modified dental amalgam alloy samples. Moreover, the content of the dental amalgam samples was qualitative analyzed. Calibration curve for mercury was achieved with linear regression coefficient of 0.93, detection limit of 2.9 ppm and relative standard deviation (RSD %) of 7.5 % in dental amalgam samples. The obtained results show the capability of the proposed LIBS setup for in-stiu real time analysis of Hg in dental amalgam with good sensitivity and high precision.

Our Aim in Dental applications

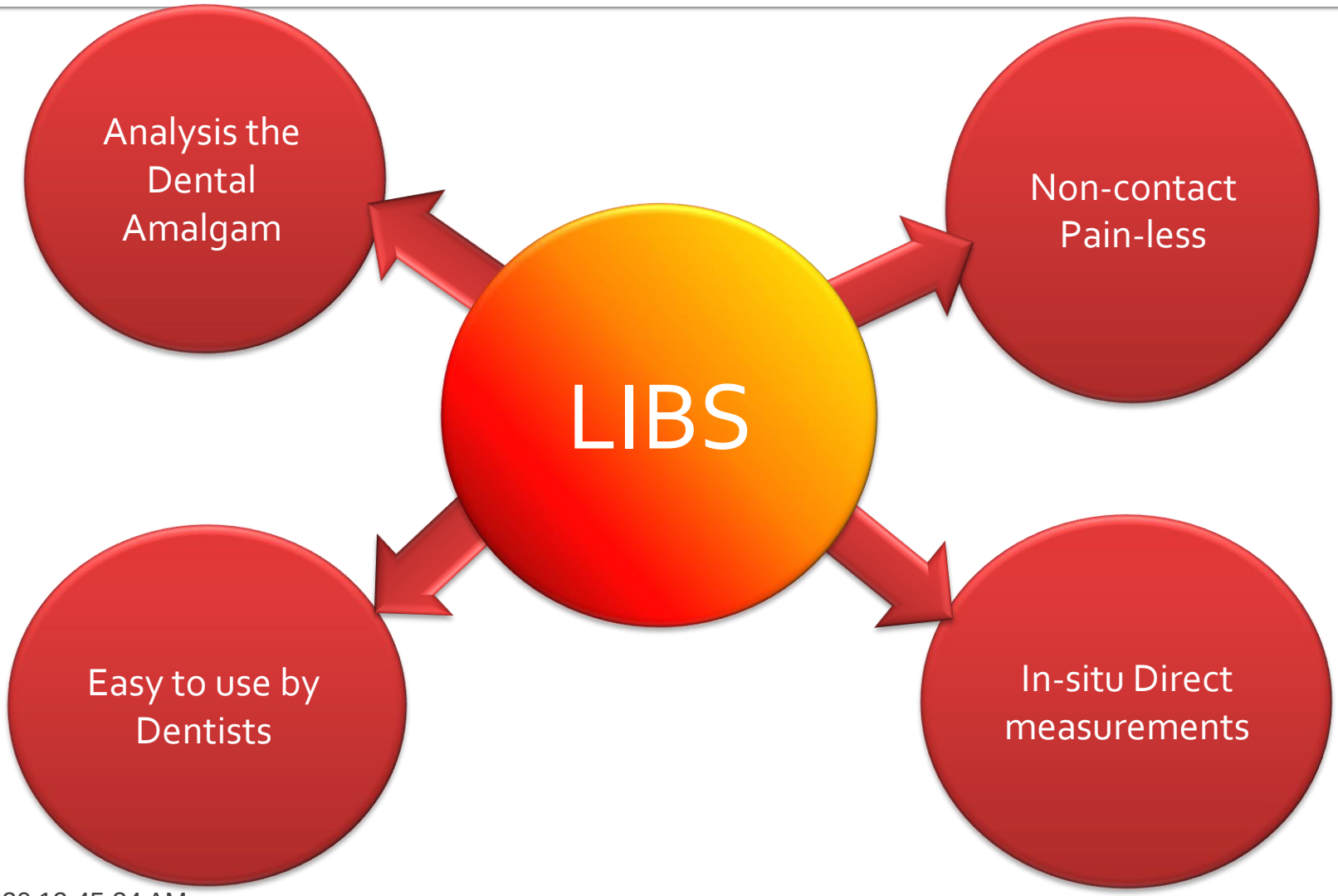

Experimental LIBS setup for analysis of Dental Amalgam

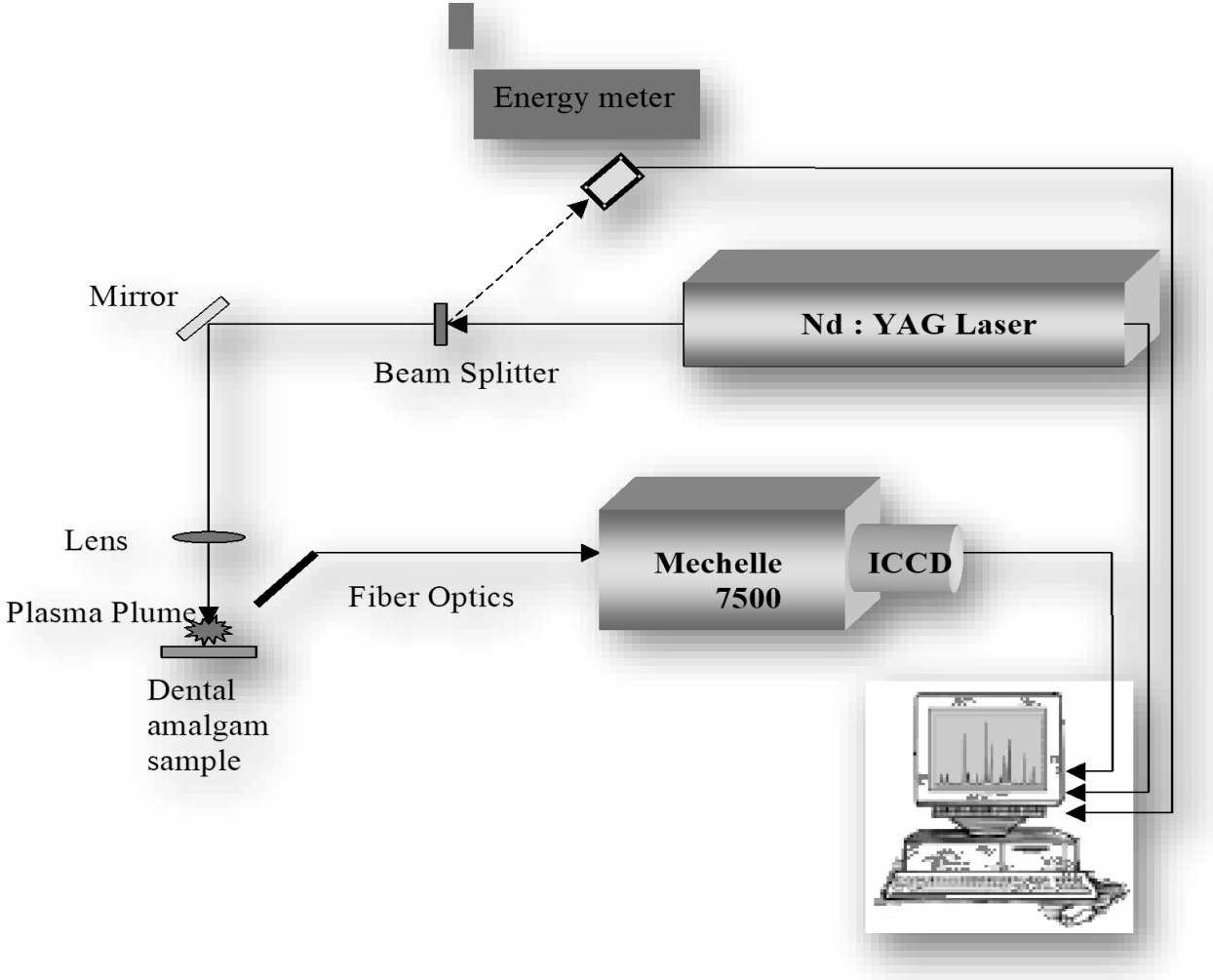

Panoramic LIBS spectrum of Dental Amalgam Sample

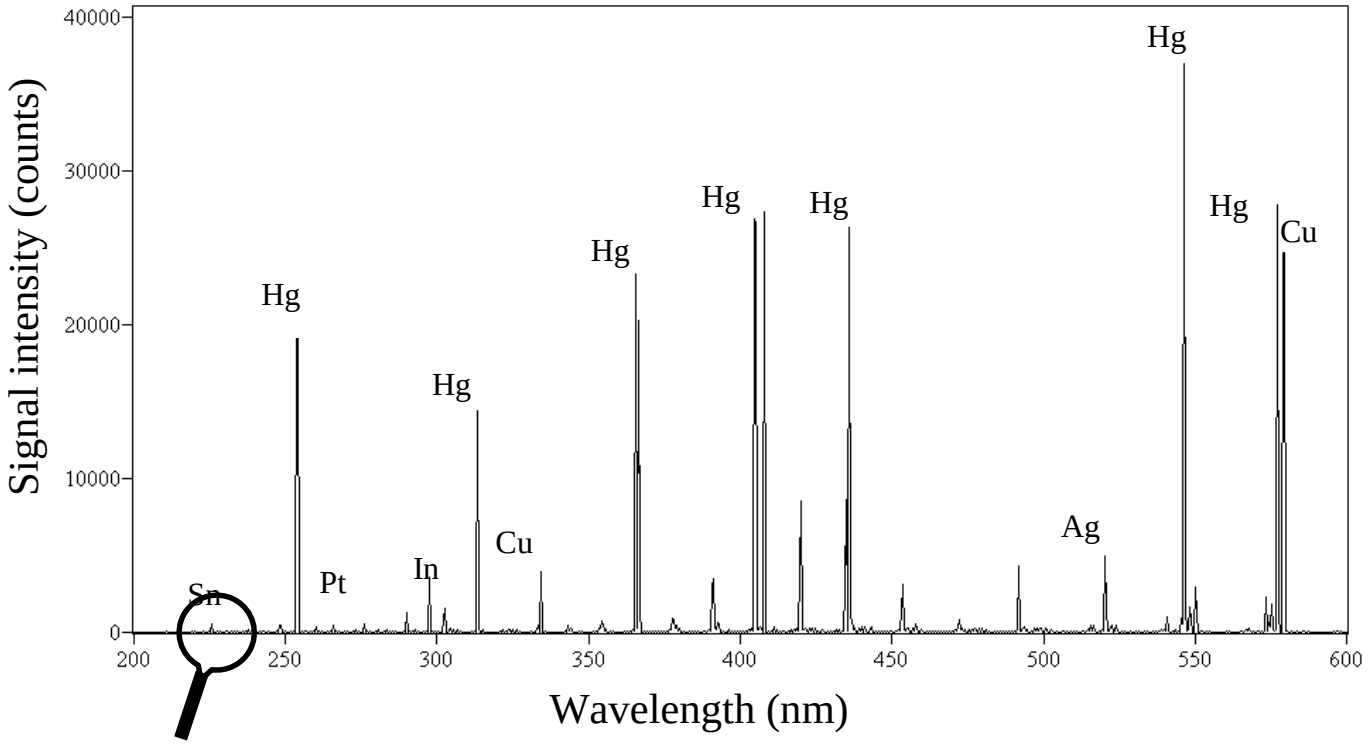

Zoomed window in the UV range 220 to 313 nm for tin at 224.67 nm with resolution of 0.04 nm ($\lambda/\Delta\lambda$ = 5617) and signal to noise ratio SNR = 9.8 in the dental amalgam sample.

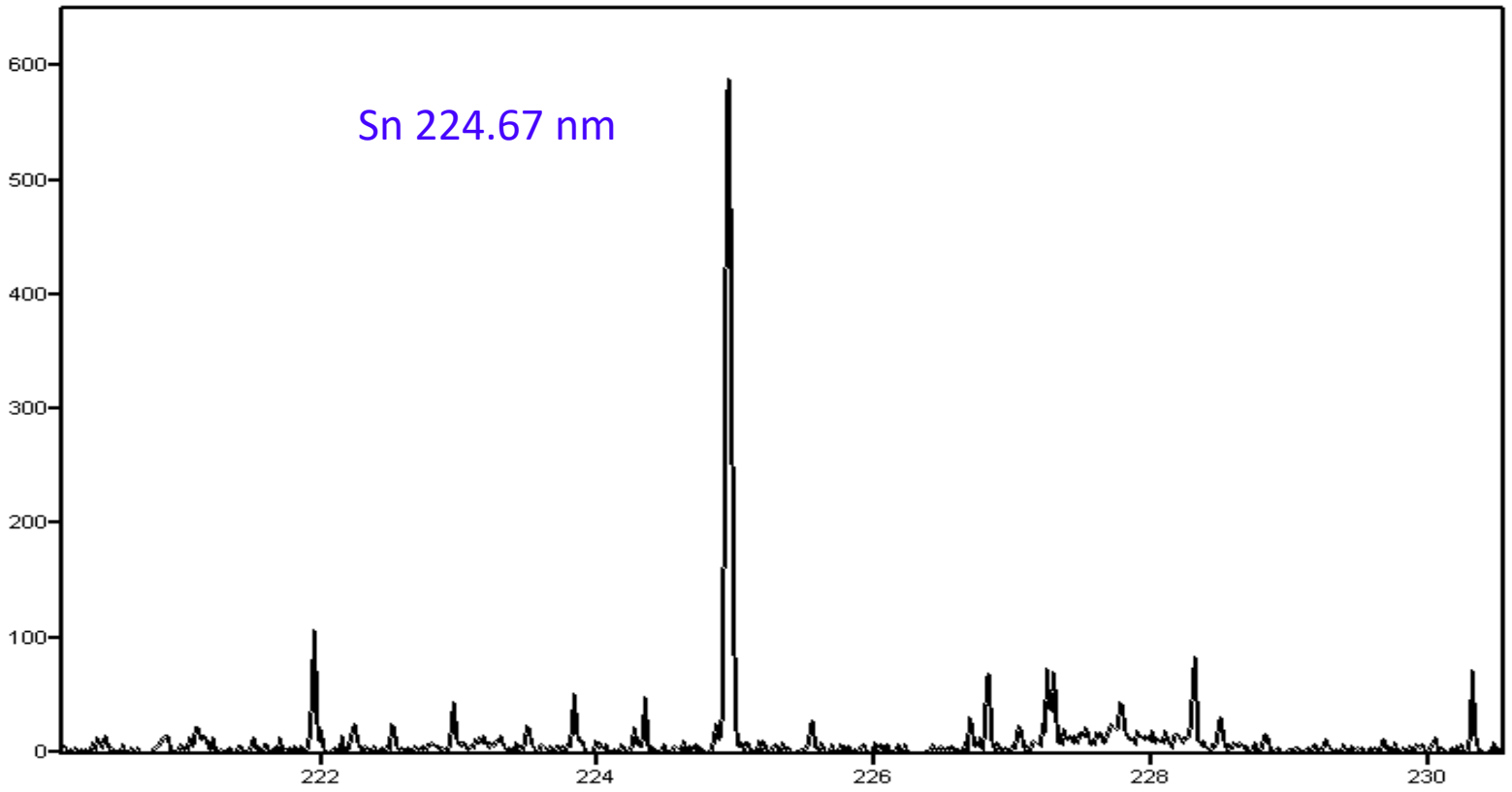

Calibration curve obtained for Mercury in Dental Amalgam

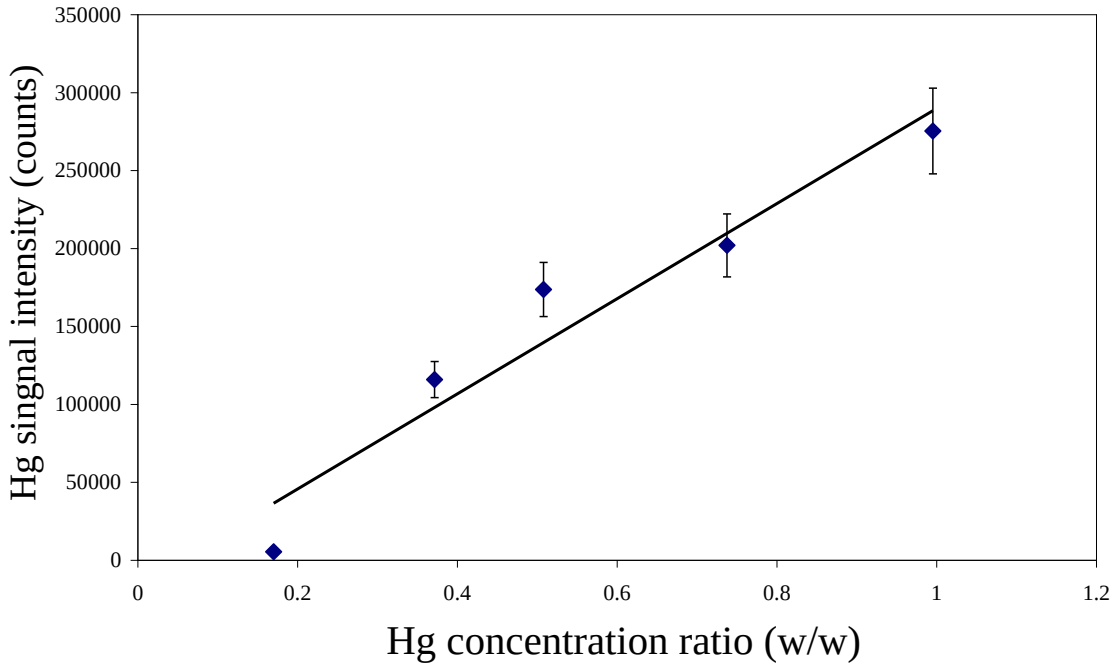

LIBS detection limit of Mercury

2.9 ppm

CONCLUSION

In summary, we have carried out an accurate LIBS setup using portable commercial Echelle spectrometer equipped with ICCD detector for qualitative analysis of platinum dental amalgam alloy samples. Mercury is quantitatively analyzed with good sensitivity and high precision.

Moreover, the proposed LIBS setup represents non-contact technique capable of remotely analyzed the dental amalgam samples contents in few minutes using one meter length fused-silica optical fiber. All of these, facilitate it to be used for in-situ real time medical applications monitoring and follow up mercury content in dental amalgam alloy.

Environmental applications Papers

Seawater

Agriculture Drainage Water

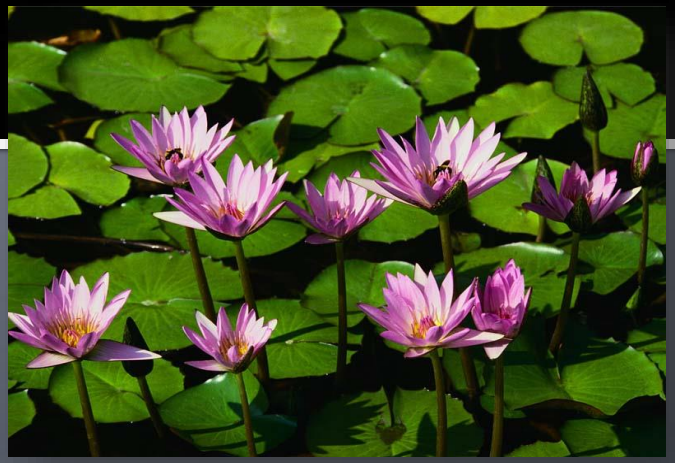

paper (8)
Quantitative elemental analysis of seawater by laser induced breakdown spectroscopy

Abstract

LIBS has been used for the determination of amounts of Ca, Na, and Mg in seawater. A specific set-up using a pulsed Q-switched Nd:YAG laser (1064 nm) focused with a tilted angle on the surface of the liquid is presented. A combination of Echelle spectrometer with a time gated intensified charge coupled device camera (ICCD) facilitated such working conditions. Multi-elemental panoramic line spectra (250 – 750 nm) have been analyzed at 1500 ns delay time and 10 µs gate width of the time window of observation. The observed wide range spectrum for seawater sample reveals strong and well resolved spectral lines for Ca, Na and Mg elements and hydrogen Hα line as well. The natural seawater sample was diluted to observe a wide range of concentrations for these elements. The corresponding calibration curves are constructed and normalized against the Hα line according to the internal standardization method. The obtained calibration curves show good linearity within two orders of magnitude. The observed detection limits were 1.6 µg/ml for Mg , 2.21 µg/ml for Ca and 30 µg/ml for Na. Exploiting the LIBS technique with an Echelle spectrometer allows for on-line quantitative measurements with good reliability and reproducibility of seawater content.

Problems in applying LIBS in liquid samples

1- The plasma expansion leads to water splashing covering the focusing optics with droplets and blocking the laser beam

solution

tilted configuration with angle 45° minimize this problem.

2- The plasma expansion generates shock waves which produced ripples on the water surface (change the focusing point)

solution

a low laser pulse repetition rate of 0.2 Hz minimize this phenomenon

Steps

1- Applying the modified LIBS setup and the possible enhancement conditions to increase the SNR.

2- verify that we have suitable spectral bandwidth.

3- Dilute the natural seawater to get several samples to build calibration curves.

4- Applying the internal standardization method to get linear calibration curves.

5- Determine LOD for seawater and compare with literature.

LIBS setup for liquid samples

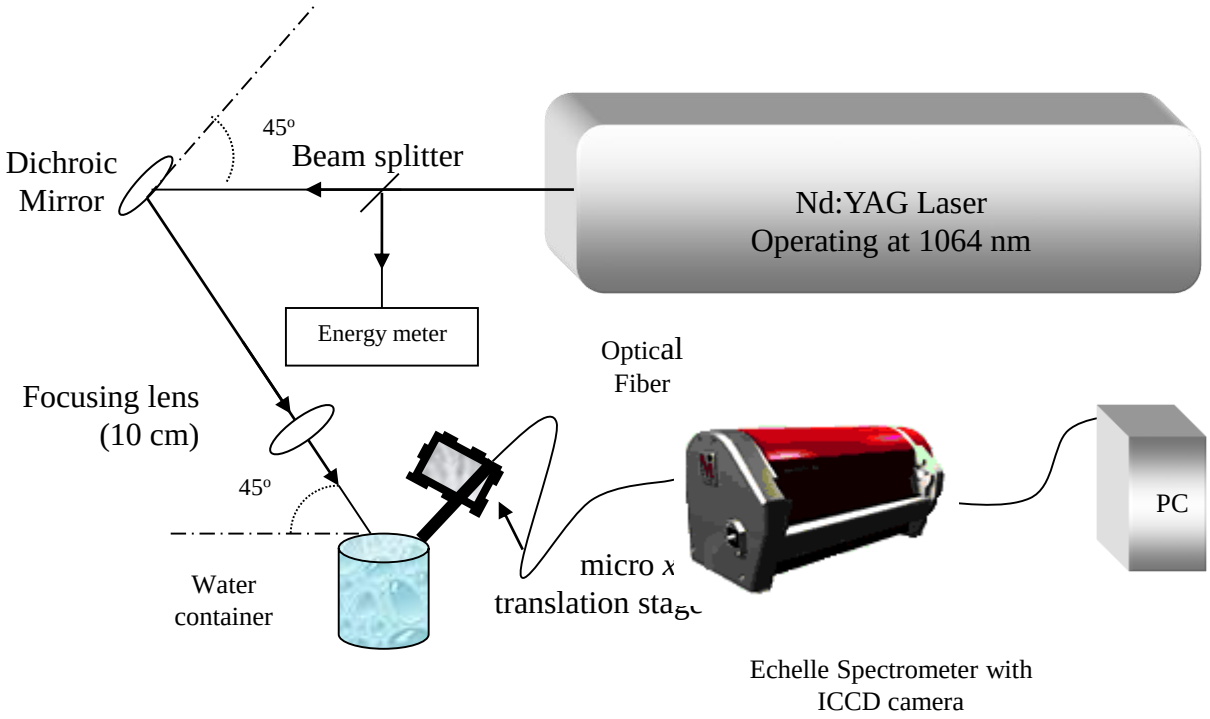

Echelle Spectrum of Sea Water

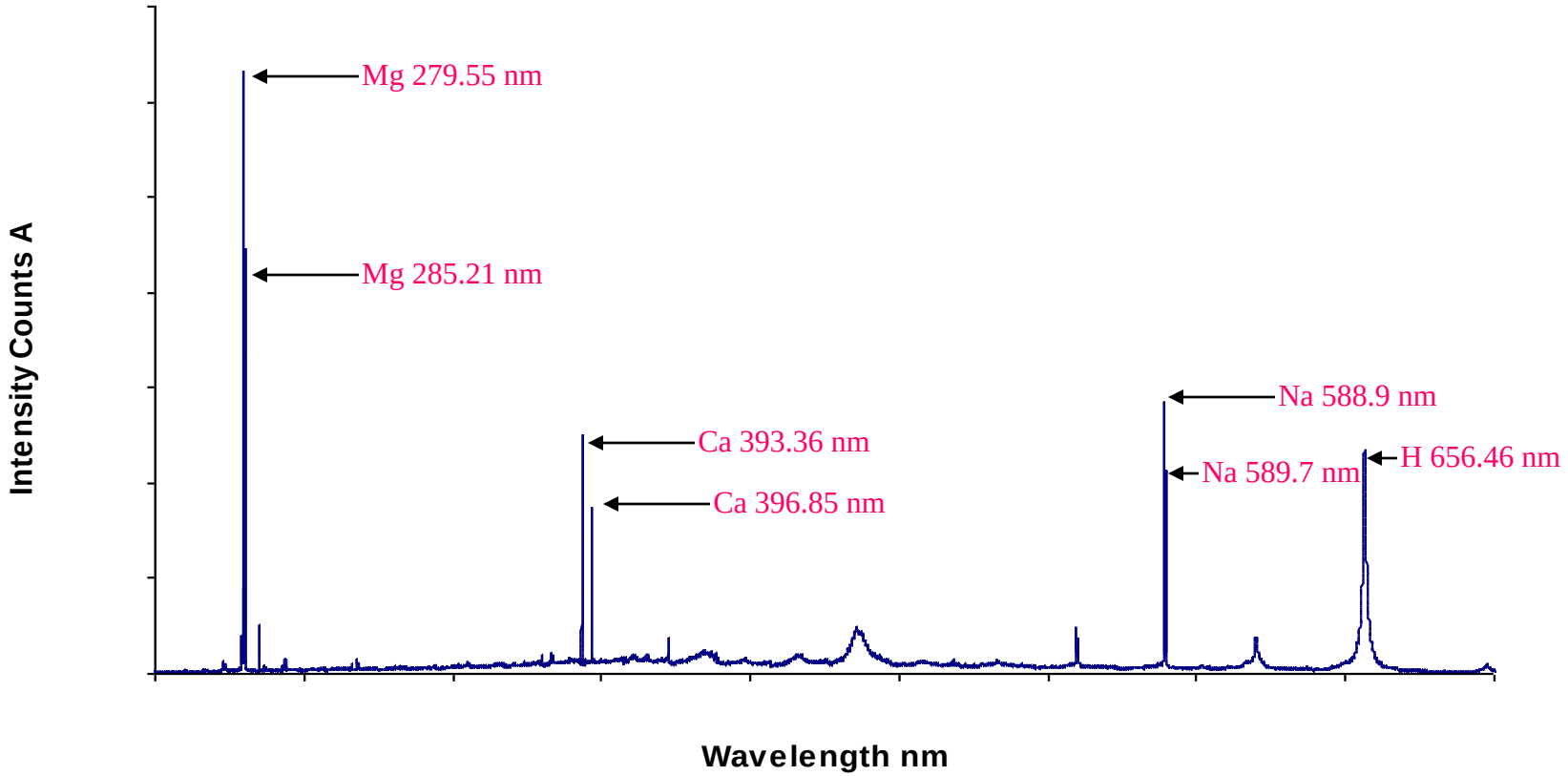

Echelle Spectra of Diluted Sea Water

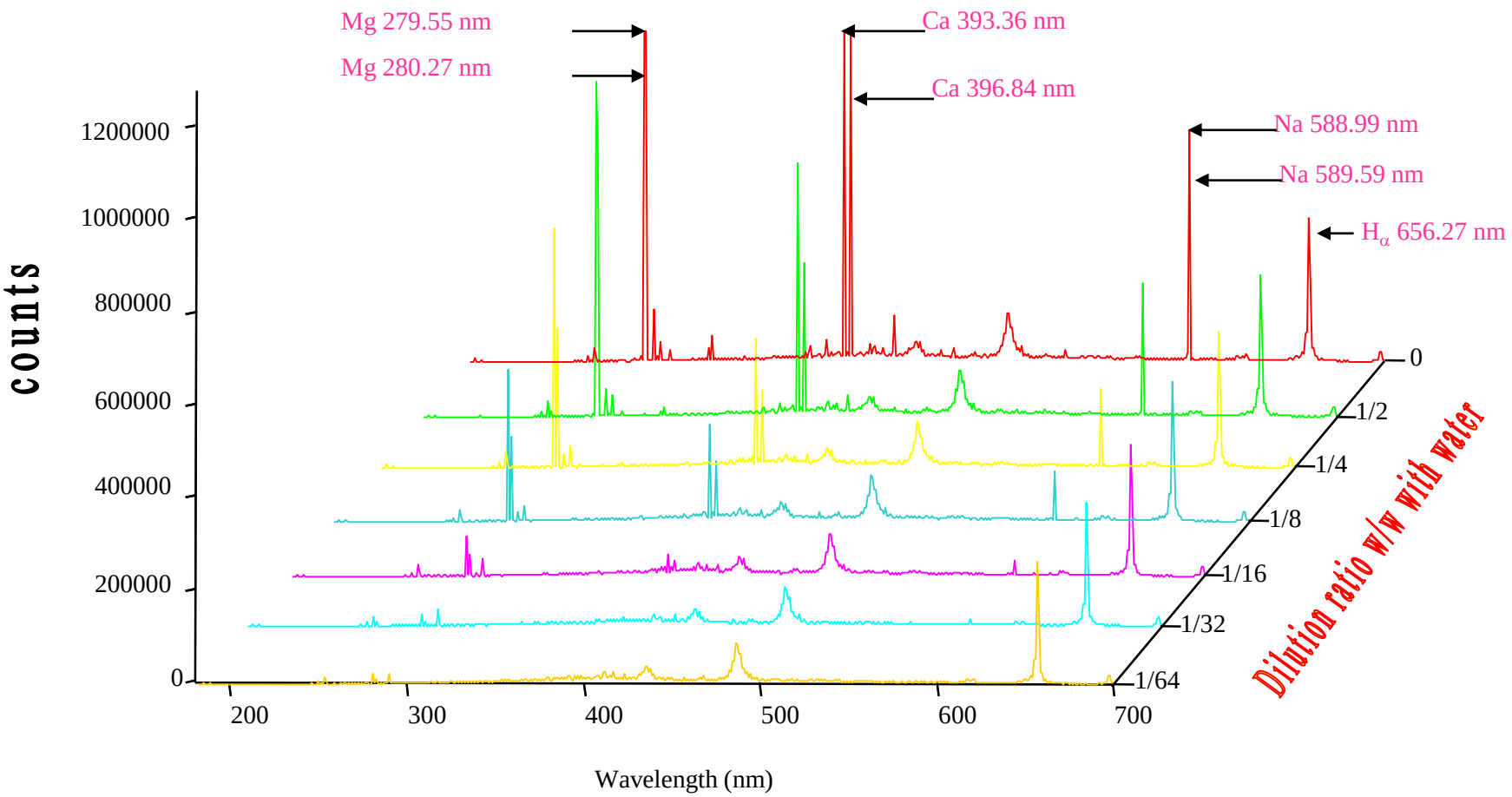

Sodium calibration curve in sea water

Internal

Standardization

non-normalized

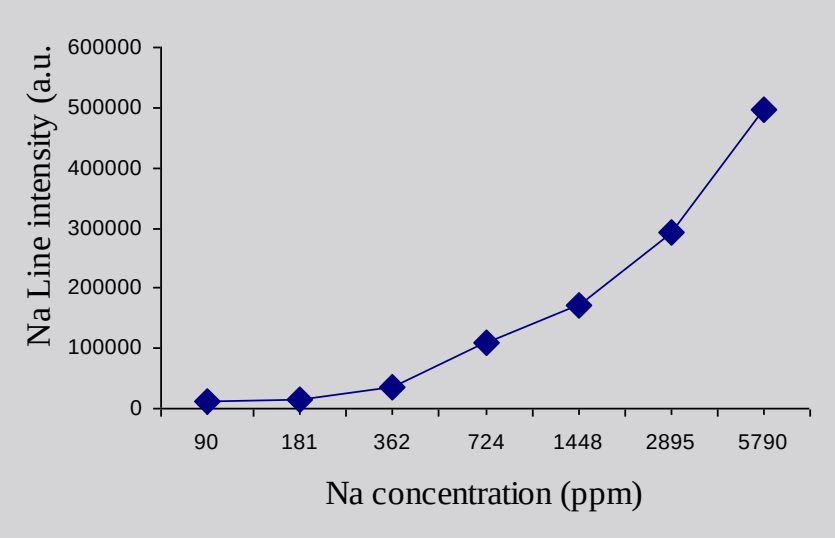

normalized

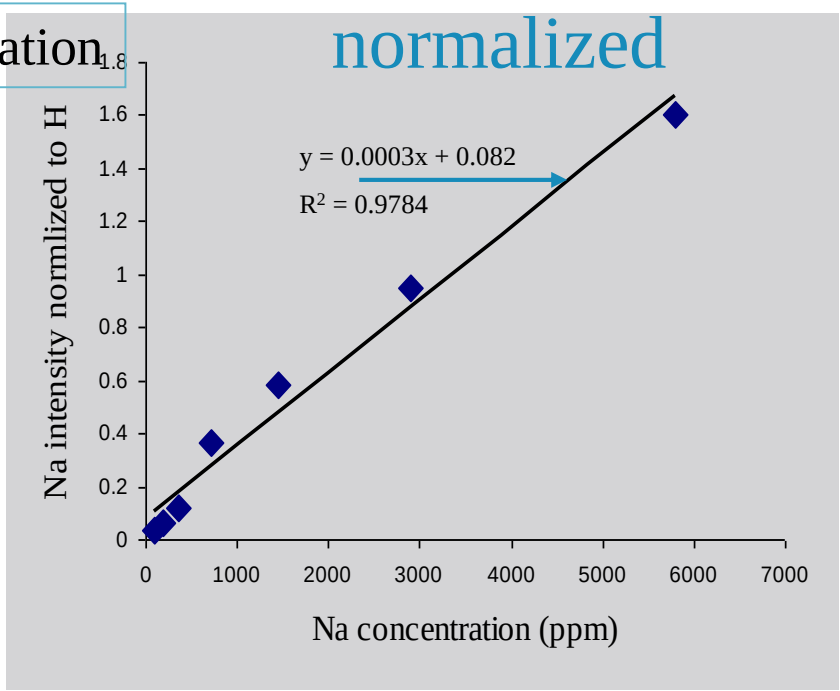

Calcium calibration curve in sea water

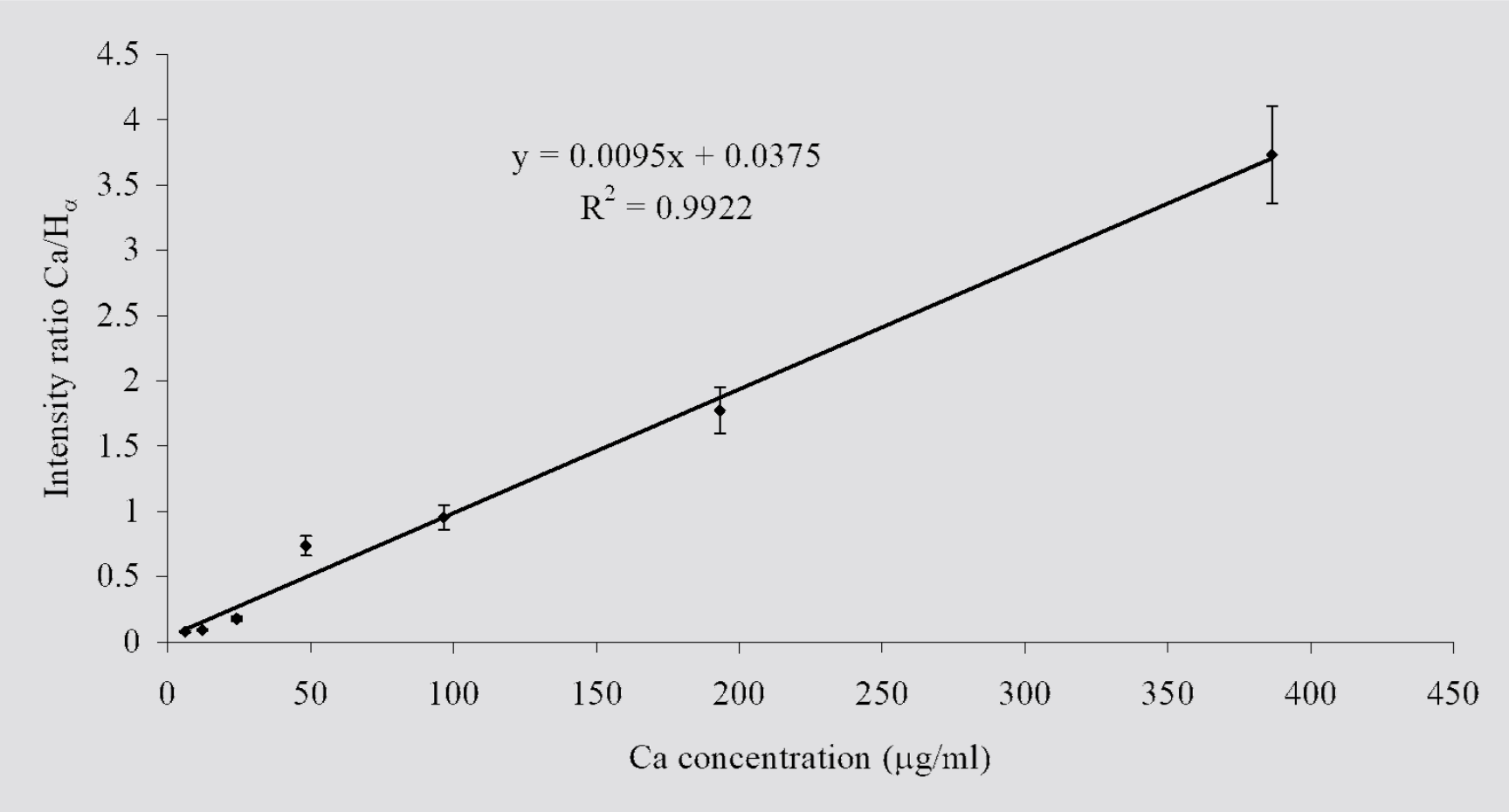

Magnesium calibration curve in sea water

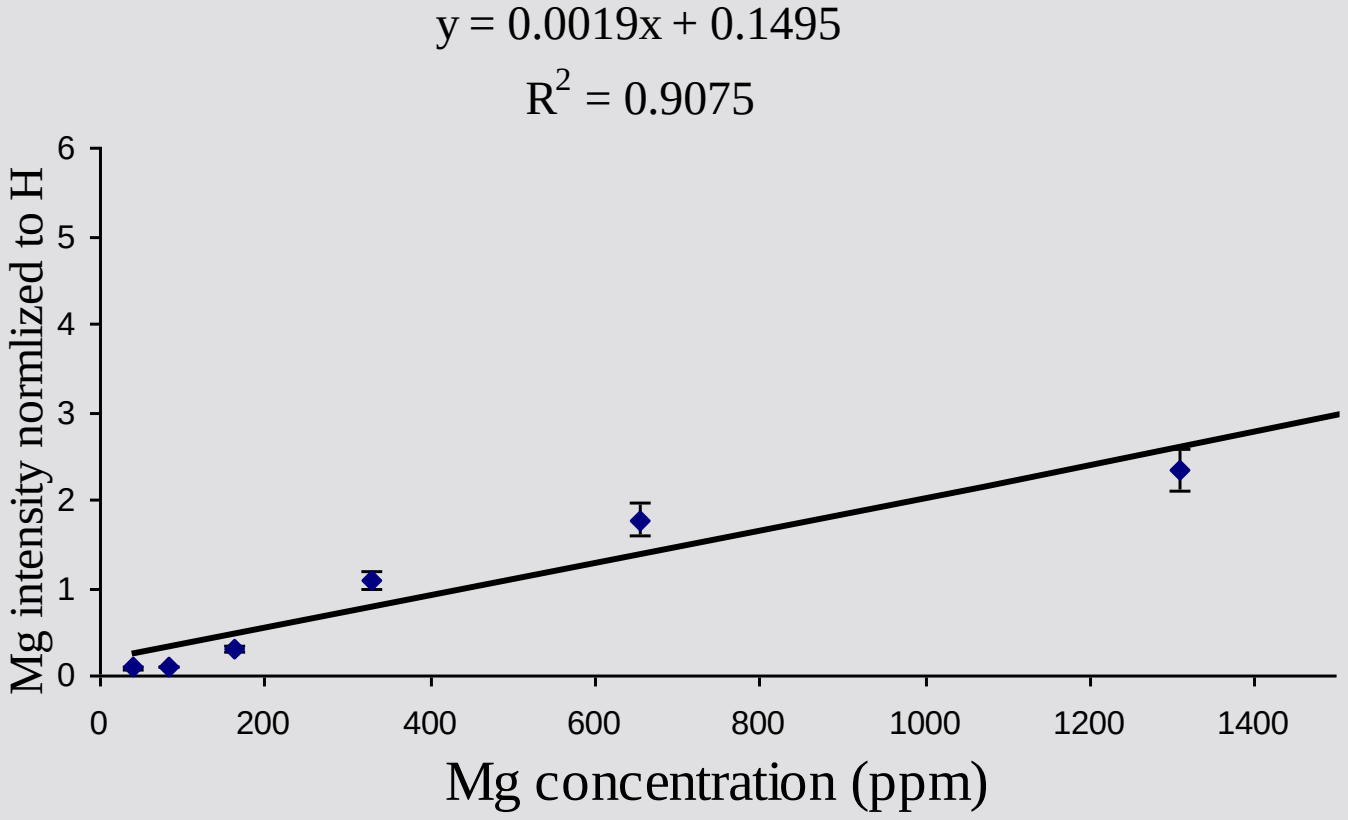

Limits of detection of Mg , Na and Ca in seawater

ELEMENT	Present work (µg/ml)	P. Fichet et al.[11] (µg/ml)
Mg	1.6	1
Na	10	0.5
Ca	2.21	0.3

Fichet et al. used a very complicated setup consists of traditional high sensitive large spectrometer of 100 cm length and 2400groves/mm attached to ICCD camera to analysis eleven elements in water. They used a standard aqueous solution for each element separately. So, they do not have any matrix effects. But, in our case, working with real natural samples, the elements are mixed in natural seawater sample which results in the matrix effect. The matrix effect in turn increases the limit of detection values as shown in this table.

Conclusion

we demonstrated a transportable LIBS setup with a portable Echelle spectrometer (30 cm length including the ICCD camera) that facilitates the quantitative measurements of Na, Ca, and Mg on the surface of seawater samples. This represents an advantage that the observed LOD values, using the proposed LIBS setup, are near to the previously published results that used a complicated setup. This facilitates our proposed LIBS setup for in-situ measurements in natural seawater.

Paper (5)

Calibration Free LIBS Identification of Seawater Salinity

Abstract

Laser-induced breakdown spectroscopy (LIBS) has been used as a remote sensing system to analysis seawater samples and identifies their salinities. The obtained values of electron temperature T_e and electron density N_e for the generated plasma on the natural seawater surface (salinity 3.753%) are 11580 K $\pm$ 0.35% and 3.33 x 10^{18} cm^{-3} $\pm$ 14.3% and have significant change only if the salinity changes. It is concluded that Te and Ne represent a fingerprint plasma characterization for a given seawater salinity.

Detailed composition of seawater at 3.5% salinity

The salinity measurement is a total of all the salts that are dissolved in the water .

Element	ppm
Sodium NaCl	10,800
Chlorine NaCl	19,400
Magnesium Mg	1,290
Sulfur S	904
Potassium K	392
Calcium Ca	411
Bromine Br	67.3
Carbon C	28
Nitrogen ion	15.5
Fluorine F	13
Boron B	4.45
Silicon Si	2.9
Phosphorus P	0.088
Iodine I	0.064
other	<0.03

Steps

1- Applying the modified setup and the possible enhancement conditions to increase the SNR.

2- verify that we have suitable spectral resolution.

3- Finding the plasma temperature T_e and density N_e for different seawater salinities .

4- Study the dependency between the obtained plasma parameters and if they change with the salinity.

Sodium lines in sea water using laser irradiance of 10^{10} W/cm^2

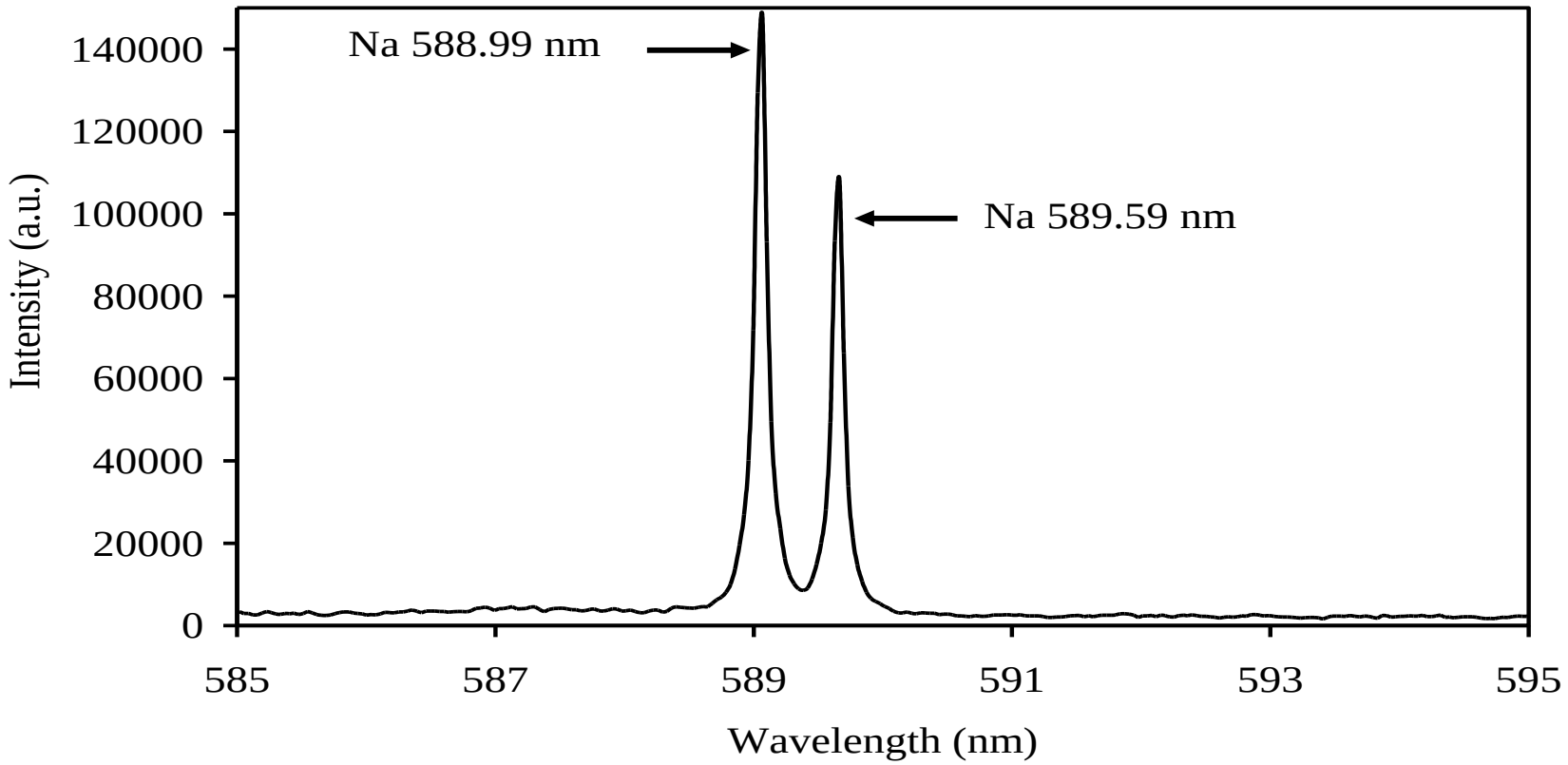

T a b l e 2. A list of the spectroscopic data of the spectral lines used for the determination of plasma temperature and density of seawater samples.

Element	Wavelength [nm]	A_{ki} [s^{-1}]	E_k [cm^{-1}]	g_k
Ca	315.89	3.10×10^{8}	56839.25	4
Ca	317.93	3.60×10^{8}	56858.46	6
Ca	373.69	1.70×10^{8}	52166.93	2
Ca	393.37	1.47×10^{8}	25414.40	4
Ca	396.85	1.40×10^{8}	25191.51	2
Ca	409.71	9.90×10^{6}	84933.65	4
Ca	410.98	1.20×10^{7}	84936.41	6
Ca	422.01	8.50×10^{6}	84300.89	2
Ca	422.67	2.18×10^{8}	23652.30	3
Ca	445.48	8.70×10^{7}	37757.45	7
Ca	500.15	2.00×10^{7}	80521.53	4
Ca	502.00	2.30×10^{7}	80526.16	6
Ca	530.72	1.50×10^{7}	79448.28	2
Ca	585.75	6.60×10^{7}	40719.85	5
Ca	643.91	5.30×10^{7}	35896.89	9
Ca	646.26	4.70×10^{7}	35818.71	7
Ca	649.38	4.40×10^{7}	35730.45	5
Ca	616.22	4.77×10^{7}	31539.49	3
Ca	644.98	9.00×10^{6}	35835.41	5
Ca	445.59	2.00×10^{7}	37751.87	5
Ca	616.96	1.90×10^{7}	36575.12	5
Ca	558.88	4.90×10^{7}	38259.12	7
Ca	559.45	3.80×10^{7}	38219.12	5
Ca	616.91	1.70×10^{7}	36554.75	3
Mg	277.66	1.32×10^{8}	57873.94	5
Mg	277.82	1.82×10^{8}	57833.40	3
Mg	277.98	4.09×10^{8}	57873.94	5
Mg	278.14	5.43×10^{8}	57812.77	1
Mg	278.29	2.14×10^{8}	57833.40	3
Mg	279.07	4.01×10^{8}	71491.06	4
Mg	279.55	2.60×10^{8}	35760.88	4

Element	Wavelength [nm]	A_{ki} [s^{-1}]	E_k [cm^{-1}]	g_k
Mg	279.79	4.79×10^{8}	71490.19	6
Mg	280.27	2.57×10^{8}	35669.31	2
Mg	281.11	1.96×10^{8}	83520.47	5
Mg	281.17	2.11×10^{8}	83511.25	3
Mg	285.21	4.91×10^{8}	35051.26	3
Mg	291.54	4.09×10^{8}	80693.01	5
Mg	292.86	1.15×10^{8}	69804.95	2
Mg	293.65	2.30×10^{8}	69804.95	2
Na	250.80	4.50×10^{9}	399177.75	10
Na	251.03	2.19×10^{8}	406865.11	2
Na	253.03	3.65×10^{7}	406550.63	4
Na	253.15	8.44×10^{7}	332710.11	4
Na	254.28	3.39×10^{7}	406865.11	2
Na	259.50	3.71×10^{7}	331745.06	3
Na	266.10	1.65×10^{8}	330789.05	5
Na	267.18	2.64×10^{8}	330636.75	3
Na	267.72	1.41×10^{10}	373981.52	6
Na	267.81	3.01×10^{8}	330549.35	1
Na	282.99	3.36×10^{7}	332962.75	5
Na	283.96	1.11×10^{8}	332841.93	7
Na	288.14	2.50×10^{8}	300387.82	1
Na	288.63	1.07×10^{8}	332802.21	5
Na	289.40	1.48×10^{8}	332710.11	1
Na	589.00	6.16×10^{7}	16973.37	4
Na	589.59	6.14×10^{7}	16956.17	2

The electron temperature Te determined from the observed sodium, calcium, and magnesium spectral lines in different seawater samples with different salinities

Na for Sample-1

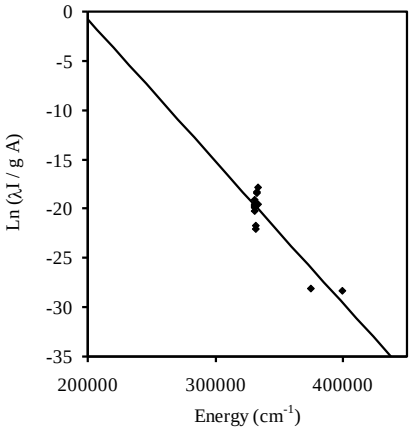

Ca for Sample-1

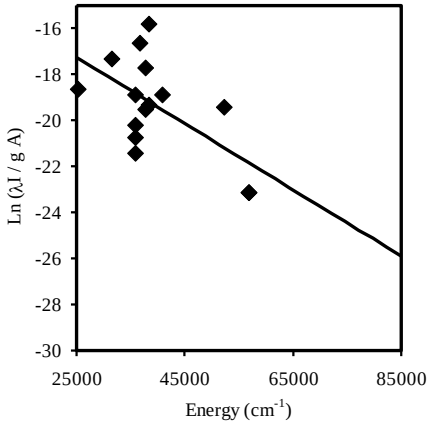

Mg for Sample-1

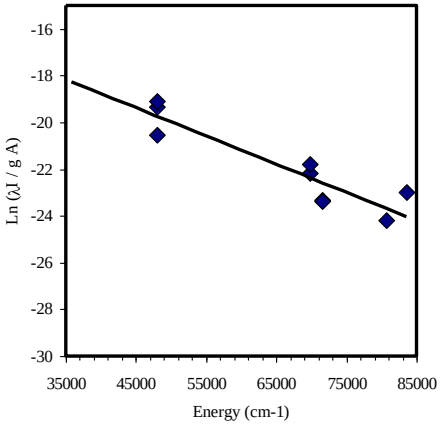

Na for Sample-2

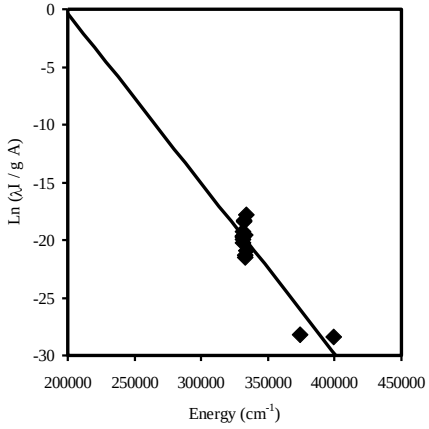

Ca for Sample-2

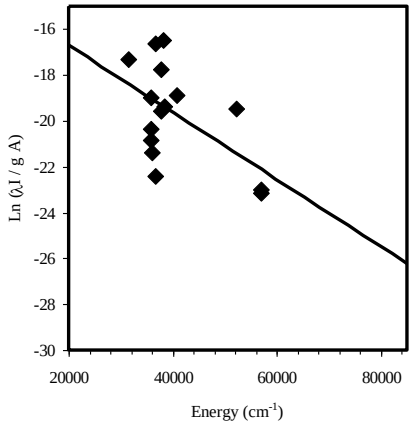

Mg for Sample-2

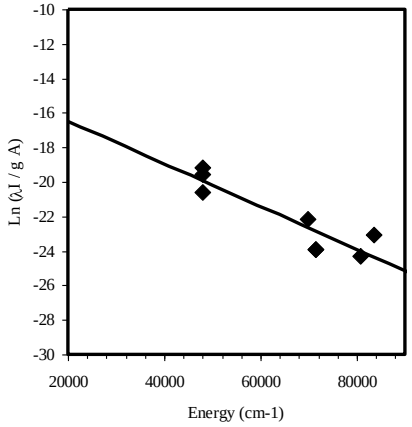

Tables of the electron temperature Te and Electron density Ne determined from the observed sodium, calcium, and magnesium spectral lines in different seawater samples with different salinities

Element	Sample-1 (salinity 3.753%)	Sample-2 (salinity 1.876%)	Sample-3 (salinity 0.938%)
Mg	11603 K	10697 K	9900 K
Ca	11547 K	10681 K	9983 K
Na	11575 K	10665 K	9943 K
Average temperature	11580 K ± 0.35%	10680 K ± 0.37%	9940 K ± 0.43%

Element	Wavelength (nm)	Stark broadening parameter (nm)	Sample-1 (salinity 3.753%) (cm^{-3})	Sample-2 (salinity 1.876%) (cm^{-3})	Sample-3 (salinity 0.938%) (cm^{-3})
Ca	422.67	7.18×10^{-4}	3.75×10^{18}	6.05×10^{17}	2.42×10^{17}
Mg	285.21	4.13×10^{-4}	2.85×10^{18}	5.92×10^{17}	2.78×10^{17}
Na	297.50	8.85×10^{-5}	3.38×10^{18}	6.21×10^{17}	2.82×10^{17}
Average N_e			$3.33 \times 10^{18} \pm 14.3\%$	$6.03 \times 10^{17} \pm 2.6\%$	$2.67 \times 10^{17} \pm 9.4\%$

3/2
12:45:35 AM

Conclusion

In the present work, we used an accurate LIBS setup to identify different seawater samples (with different salinities) using an optical fiber probe. In doing so, we study the matrix effect on the plasma characterization of seawater samples. The obtained results showed that both electron temperature and density are related to the matrix composition and change if the matrix changes. Moreover, T_e and N_e could be measured using any of the three elements (Na, Ca, and Mg) in the seawater matrix. This means that T_e and N_e represent a fingerprint plasma characterization for a given seawater sample and its salinity could be identify using only one element without needing to analysis the rest of elements in the seawater matrix. This could be done by building a database containing the determined values of T_e and N_e for a wide range of seawater salinities. Then the salinity of the unknown seawater sample could be identified just by comparing its measured T_e and N_e values with the previously stored values in our database.

The obtained results indicate that it is possible to improve the exploitation of LIBS in the remote on-line environmental monitoring, by following up only a single element as a marker to identify the seawater matrix composition and salinity without needing to analysis that matrix which saves a lot of time and efforts.

Paper (7)

Quantitative Elemental Analysis In Agriculture Drainage Water Using Laser Induced Breakdown Spectroscopy

Abstract

Application of laser induced breakdown spectroscopy (LIBS) to the qualitative and quantitative analysis of trace elements in agriculture drainage water has been considered. In the present work we are studying the effect of presence of increasing number of different salts on the limit of detection (LOD) in agriculture drainage water. The pilot area is located in the El-saff region, El-shobak, in the south of Helwan city which is the south of Cairo. This area is industrial polluted area (including an iron and steel factory, company for metallurgical work and beside coke factory). These industries produce large amounts of wastes which are dumped either into artificial canal covering large areas behind the factories or down flow through a secondary canal to El-hager. We chose 3 subsurface drainage room and 5 subsurface drainage line in the experiment in area of about 50 yokes.

HELWAN
LOCATION MAP
A·R·E
N
RIVER NILE
El-Khashab Canal
El-Hagir Canal
EL-TEBEEN
Industrial Company
Iron and steel
Factory
Out Let
OUT LET
HELWAN
SLUDGE
STATION
COKE
RIVER NILE
EL-Shobok
Khashab Canal
Arab Abou Soeid
EL-MINYA
EL-Ulayat
El-Shurafa
Arab El-Gababra
Kafr Tarkhan Canal
El-Hagir Canal
0
2.5
5km
SCALE
1 : 50.000

Elemental Analysis In Agriculture Drainage Water Using LIBS During year 2001/2002

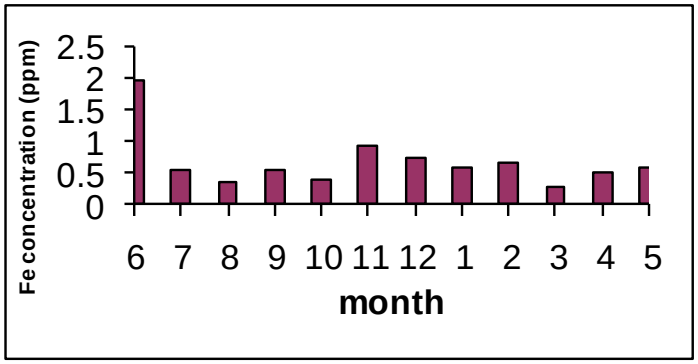

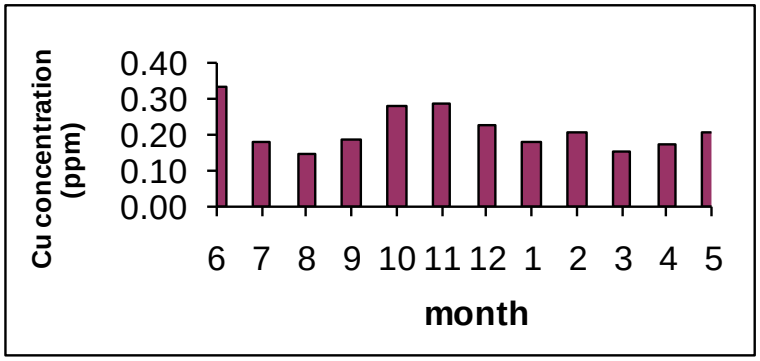

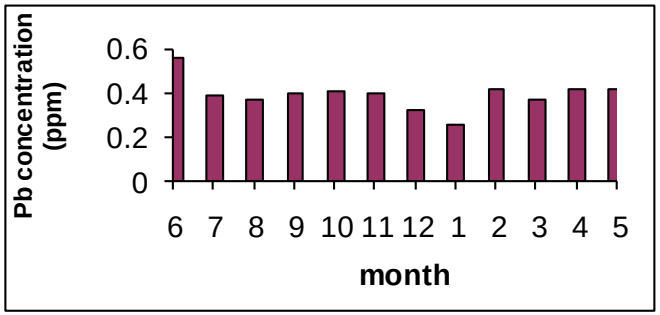

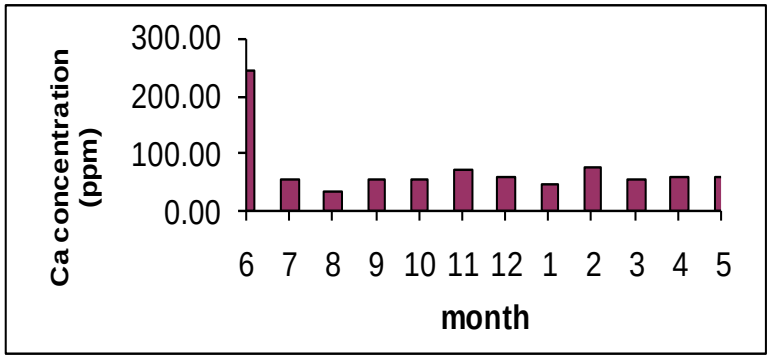

Linear calibration curves for elements in Agriculture Drainage Water samples

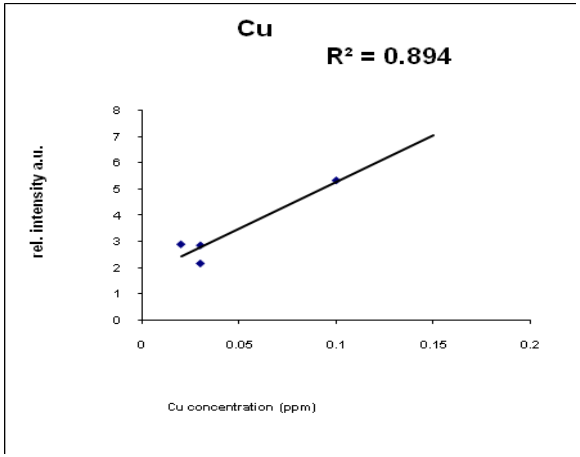

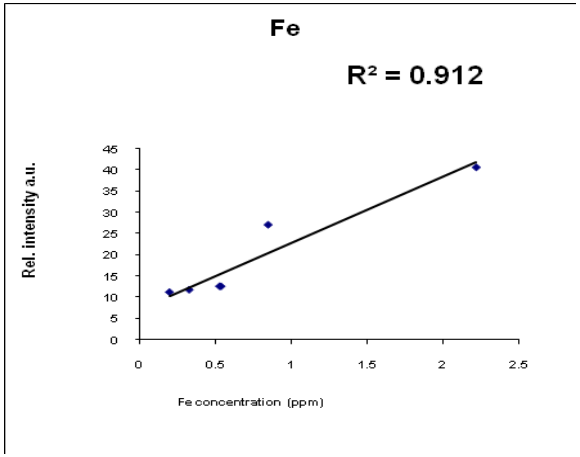

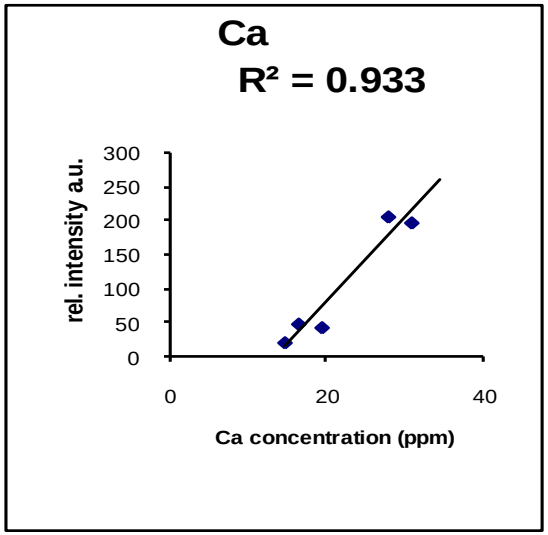

Table(1): The seven agriculture drainage water samples , which are collected from a specific agriculture field located beside a steel factory in the south of Cairo delta, were analyzed using LIBS and AAS for the iron, calcium and copper as trace elements and the average concentrations during a year are tabulated below.

Samples	Fe (ppm)		Ca (ppm)		Cu (ppm)	
	AAS	LIBS	AAS	LIBS	AAS	LIBS
Sample 1	0.85	1.27	27.89	30.2	0.1	0.1
Sample 2	0.53	0.34	16.58	17.5	0.09	0.03
Sample 3	0.54	0.34	14.84	15.28	0.02	0.05
Sample 4	0.33	0.29	19.52	17	0.15	0.016
Sample 5	0.20	0.25	31.04	17.39	0.02	0.033
Sample 6	2.22	2.1	34.75	22.73	0.03	0.032
Sample 7	0.4	0.7	30.83	29.52	0.12	0.035

Table (3): A comparison of LIBS LOD values observed for the measured elements in agriculture drainage water with the literature.

Element	Wavelength (nm)	LOD (ppm) (this work)	LOD (ppm) (literature)
Fe	373.71	0.65	30
Ca	393.36	0.15	0.3
Cu	327.70	0.10	7

CONCLUSION

Exploiting the LIBS technique with an Echelle spectrometer facilitated – for the first time- to detect toxin elements directly in natural agriculture drainage water samples collected from an industrial polluted area. This technique could measure the samples in field in real time without needing to move the samples to laboratory which saved time and efforts. Moreover, the use of an Echelle spectrometer coupled to an intensified CCD camera advantageously provided panoramic spectra extending over wide range that enables mutli-elemental analyses at once. This facilitates the normalization of the analyte spectral lines by the strong and well-resolved H_α line that improves the reliability and reproducibility of the LIBS technique compared to the conventional narrow range grating spectrometer LIBS experiments. Toxin elements, i.e. high concentrations of iron, calcium and copper were determined in natural agriculture drainage water samples with high accuracy. Also, new limits of detections of LIBS for Fe, Ca and Cu have been achieved which enables that system to be very sensitive for detecting trace elements in the ppm range of concentrations. The obtained results are great better in compare with previously obtained results by others who performed their experiments on artificial samples using conventional spectrometers with variable experimental parameters for each element.

Final Conclusion

- ✓ LIBS technique with an Echelle spectrometer could be applied as Elemental Analytical Technique in industrial applications, medical applications and environmental applications.
- ✓ LIBS could have very low LOD (< 1ppm) by applying specific optimization conditions.
- ✓ LIBS could be applied for the in field direct measurements with high precision without any sample preparation.
- ✓ LIBS offers a new method for fast identification of samples by determination of its plasma parameters without needing to build calibration curves which will save time and efforts in many applications in the near future.

FUTURE WORK :
LIBS in space exploration

Laser Induced Breakdown Spectroscopy (LIBS) is nowadays a good candidate for in-situ chemical analysis of planetary surfaces material because :

1- It can be performed on a small sample amount without any preparation.
2- It provides a multielement analysis.
3- LIBS have good sensitivity and very high spatial resolution.
4- Its depth profiling capability.
5- LIBS can remove dust layers remotely.
6- Compact instrument, with low weight, size and power consumption.

These features make the LIBS technique especially suited for a rover.

FUTURE WORK :
LIBS in space exploration

- LIBS was selected by **NASA** as part of the ChemCam instrument package for the Mars Science Laboratory rover **K9** launched in **2009** . ChemCam's Laser-Induced Breakdown Spectroscopy instrument will ablate surface coatings from materials and measure the elemental composition of underlying rocks and soils at distances from 1 up to 10 m.
- The LIBS experimental arrangement has to be optimized for space flight, and relevant minerals, rocks and soils must be tested under a simulated Mars atmosphere

FUTURE WORK :
LIBS in space exploration

The K9 rover in the field. The LIBS sensor head can be seen mounted on the right side of the mast head instrument suite. The range finder is seen as a protrusion to the right of the LIBS sensor head. Photo courtesy of NASA Ames Research Center.

FUTURE WORK :
LIBS in space exploration

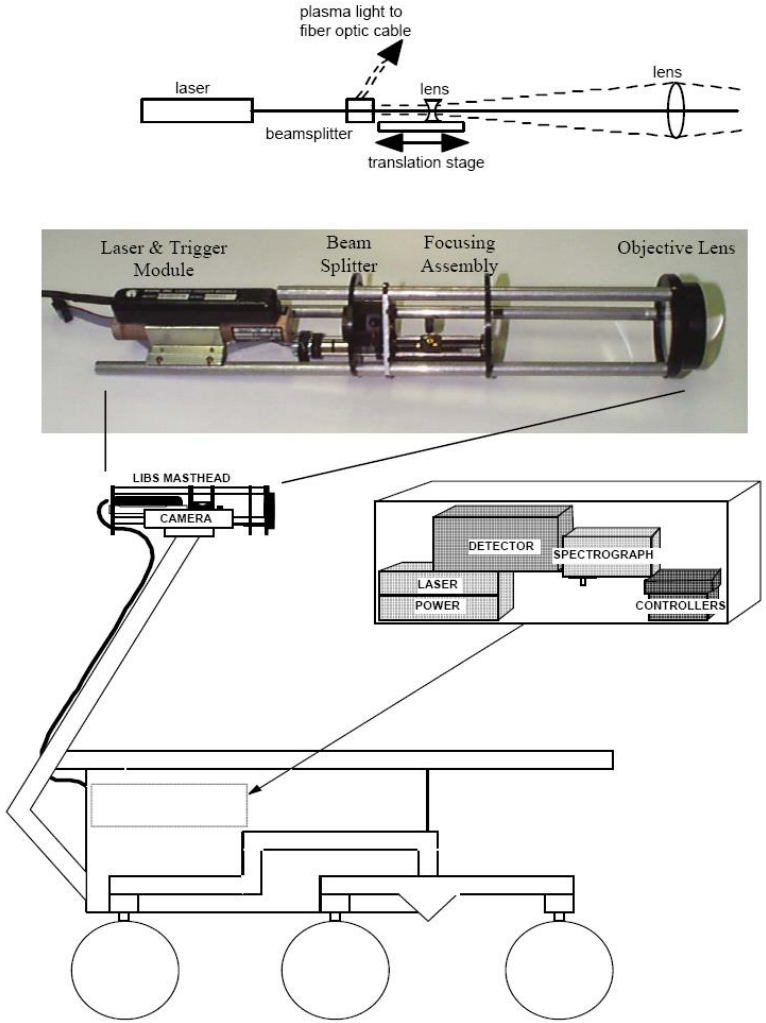

PROPOSAL: LIBS in space exploration:
simulated Martian atmosphere (~5 mbar of CO_2)

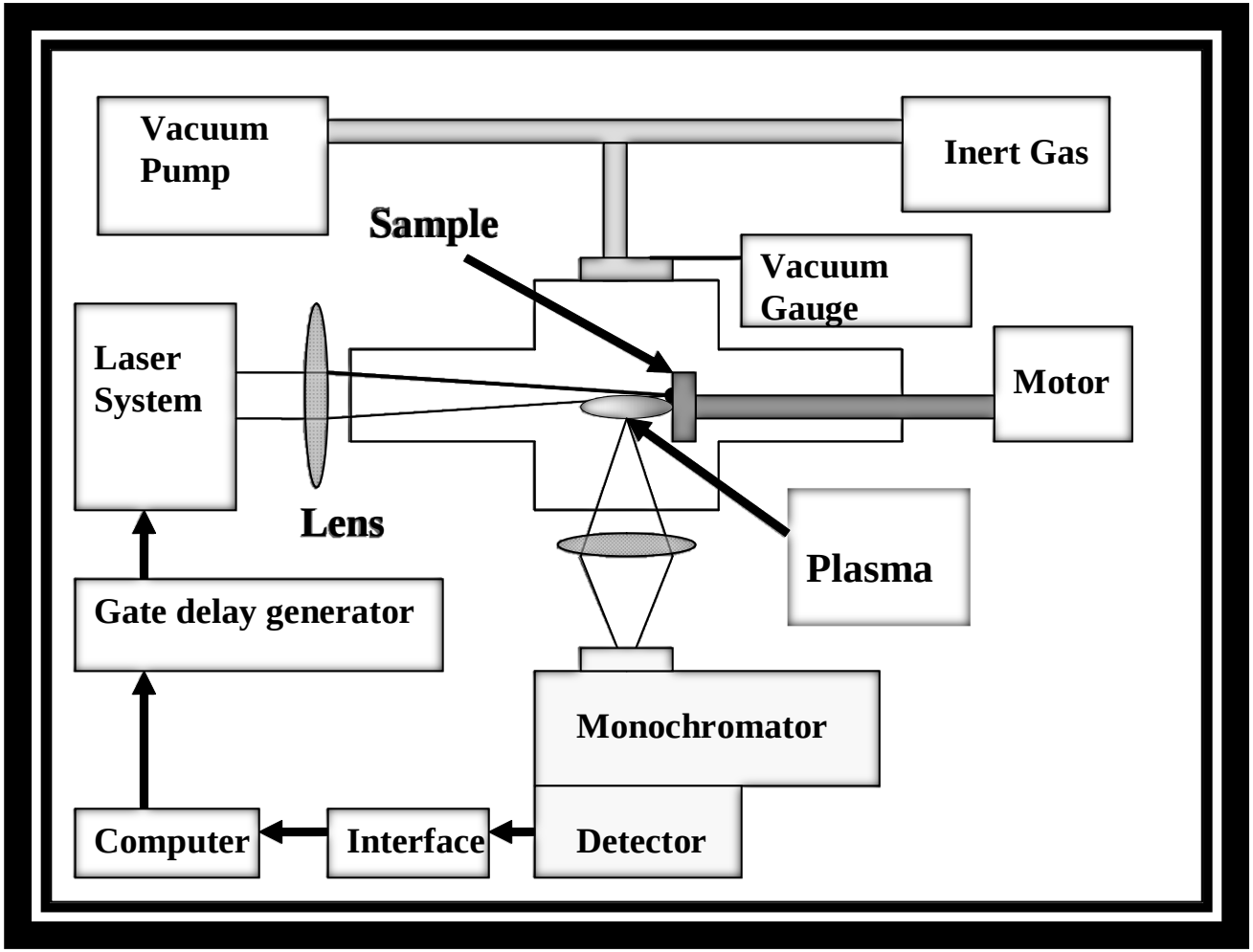

Exploring the ultrafast dynamics of a diarylethene derivative DMP using ultrafast pulses

We designed and fabricated liquid crystals of photochromic diarylethene , 1,2-bis(2-methoxy-5-phenyl-3-thienyl) perfluorocyclopentene (DMP), which exhibits photochromic reactions up to high conversion in high efficiency because the diarylethene molecule has extremely small photocycloreversion quantum yield. The liquid crystals prepared underwent photochromism upon alternating irradiation with ultraviolet and visible light. The intermolecular interaction between the photogenerated closed-ring isomers plays a significant role in deforming the Molecular structure . We investigate the origin of this behaviour by means of ultrafast transient absorption spectroscopy utilizing sub-10 fs pulses, which is an invaluable tool for simultaneously studying both the electronic and the vibrational molecular dynamics.

Arkadiusz Jarota, Ewa Pastorczak, Walid Tawfik, Bing Xue, Rafał Kania, Halina Abramczyk and Takayoshi Kobayashi "Exploring ultrafast dynamics of diarylethene derivative by sub-10 fs laser pulses " Phys. Chem. Chem. Phys., 2019,21, 192-204 ; DOI 10.1039/C8CP05882B

Exploring the ultrafast dynamics of a diarylethene derivative DMP using ultrafast pulses

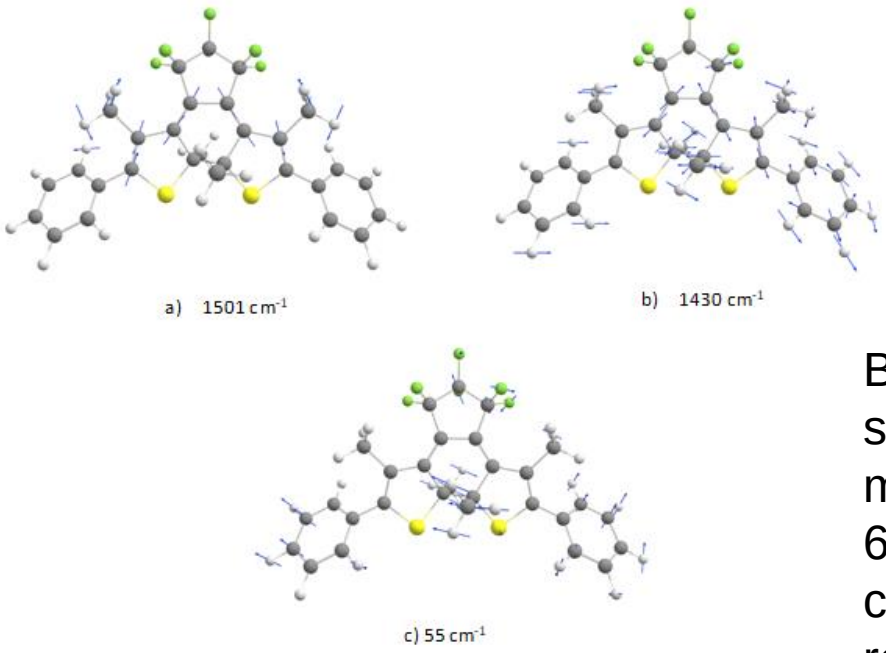

By applying ultrafast pulses in the spectral range 605 – 750 nm, the molecular vibrations of 1501, 1430 and 60 cm^{-1} are observed. Fast internal conversion S1 - S0 originates in relaxation.

Arkadiusz Jarota, Ewa Pastorczak, Walid Tawfik, Bing Xue, Rafał Kania, Halina Abramczyk and Takayoshi Kobayashi "Exploring ultrafast dynamics of diarylethene derivative by sub-10 fs laser pulses " Phys. Chem. Chem. Phys., 2019,21, 192-204 ; DOI 10.1039/C8CP05882B

Exploring the ultrafast dynamics of a diarylethene derivative DMP using ultrafast pulses

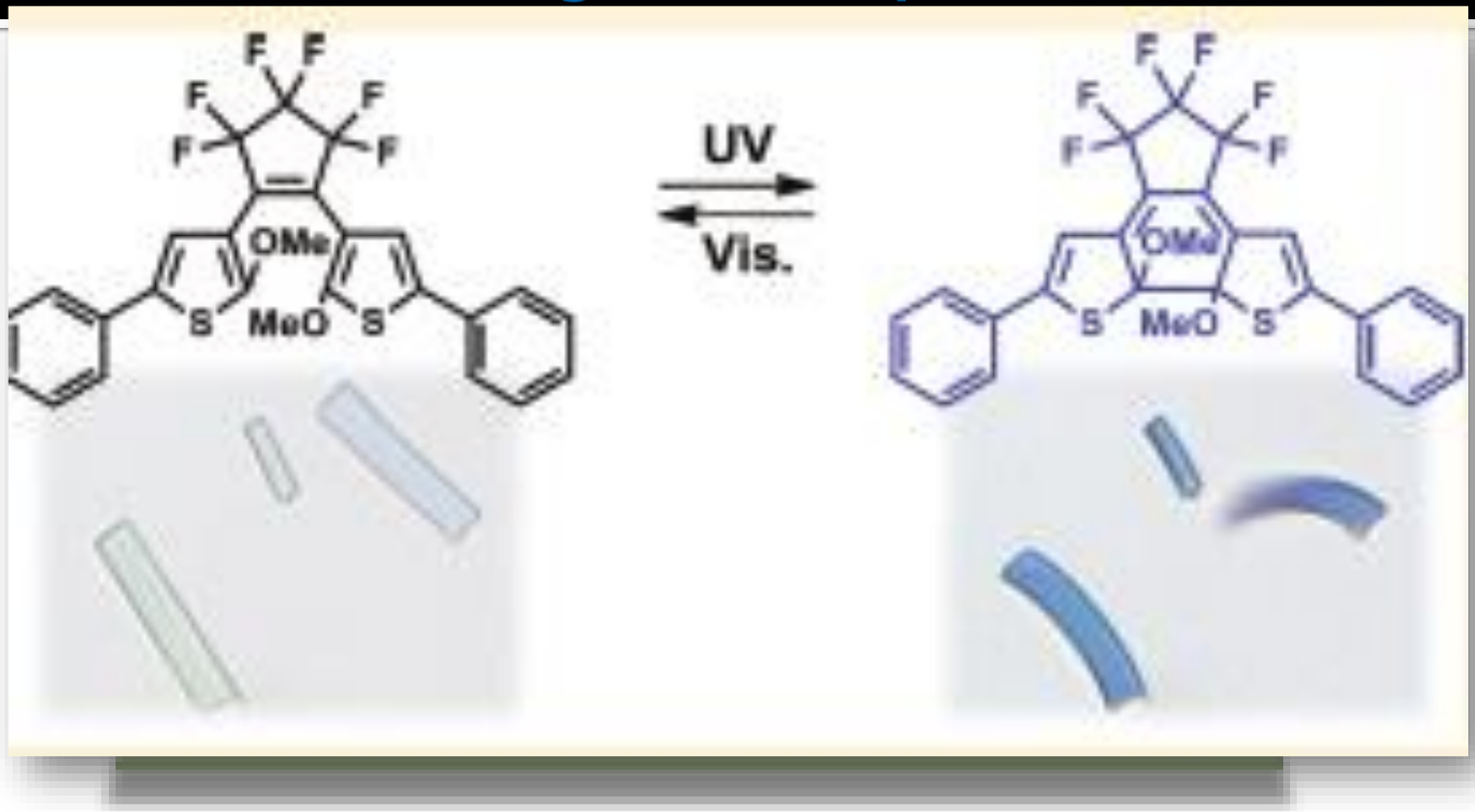

Arkadiusz Jarota, Ewa Pastorczak, Walid Tawfik, Bing Xue, Rafał Kania, Halina Abramczyk and Takayoshi Kobayashi "Exploring ultrafast dynamics of diarylethene derivative by sub-10 fs laser pulses " Phys. Chem. Chem. Phys., 2019,21, 192-204 ; DOI 10.1039/C8CP05882B

Exploring the ultrafast dynamics of a diarylethene derivative DMP using ultrafast pulses

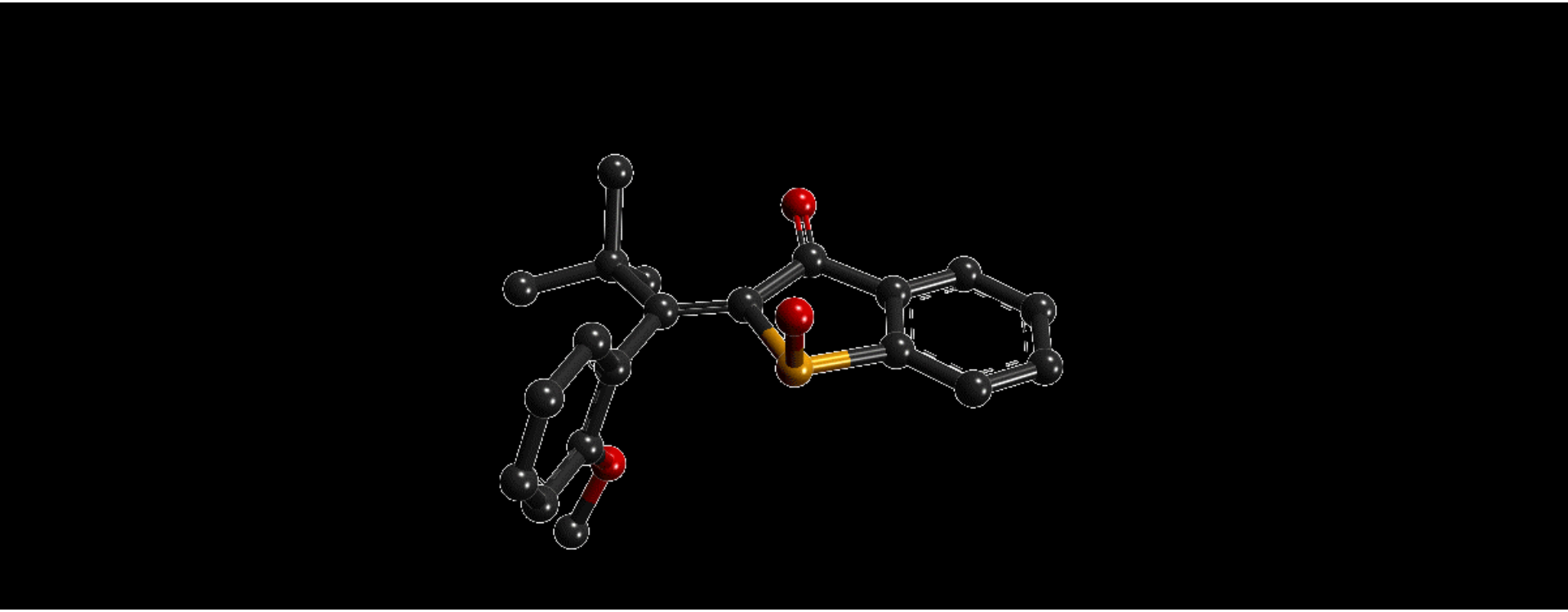

Arkadiusz Jarota, Ewa Pastorczak, Walid Tawfik, Bing Xue, Rafał Kania, Halina Abramczyk and Takayoshi Kobayashi "Exploring ultrafast dynamics of diarylethene derivative by sub-10 fs laser pulses " Phys. Chem. Chem. Phys., 2019,21, 192-204 ; DOI 10.1039/C8CP05882B

Exploring the ultrafast dynamics of a diarylethene derivative DMP using ultrafast pulses

Chemical bond rearrangement during the photo-transformation induces electronic as well as geometrical structure changes of the molecules. The molecular structure changes can be applied to various photonic devices. The electronic structure changes can be applied to optical memory media and various photoswitching devices (or molecular machines).

Arkadiusz Jarota, Ewa Pastorczak, Walid Tawfik, Bing Xue, Rafał Kania, Halina Abramczyk and Takayoshi Kobayashi "Exploring ultrafast dynamics of diarylethene derivative by sub-10 fs laser pulses " Phys. Chem. Chem. Phys., 2019,21, 192-204 ; DOI 10.1039/C8CP05882B

Application : Optical Computer Closer: Optical Transistor Made From Photo-Switch Molecule

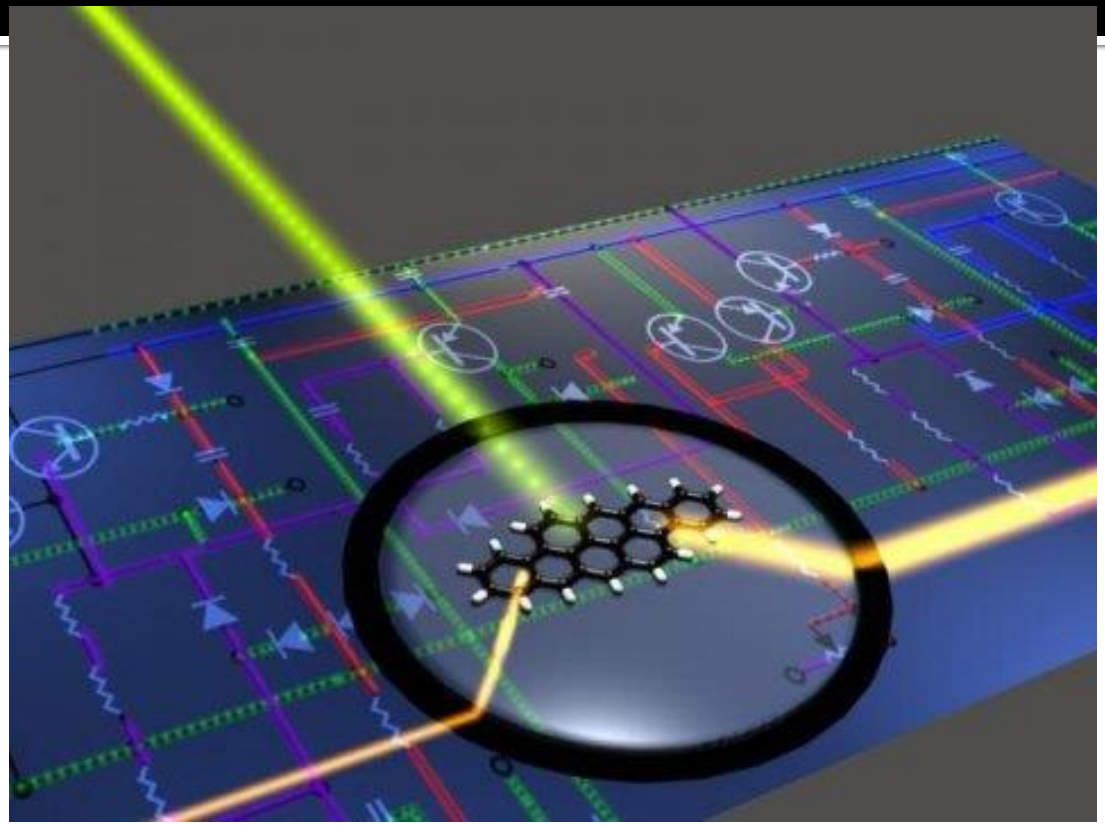

J. Hwang, M. Pototschnig, R. Lettow, G. Zumofen, A. Renn, S. Götzinger, V. Sandoghda. A single-molecule opzical transistor. Nature, 460, 76-80 DOI: 10.1038/nature08134

A photonic circuit with molecular building blocks. A single-molecule optical transistor is depicted using a standard symbol for an electronic transistor.

Conclusion

- we have demonstrated fs system which has the ability to generate pulses of 0.6 mJ with variable pulse duration from 6 fs to almost 13 fs.
- The applied method generates ultrafast pulses of with bandwidth of about 94 THz using injected pulses of about 19 THz. So, the throughput optical enhancement reaches about five-octave-wide extending from 360 - 455 THz.
- The observed results are important to control the progression of strong-electric-field interactions on the ultrafast time scale, and can be used to create more shorter pulses in the attosecond regime with shorter wavelength in the UV- x-ray regime in the forthcoming future.

Microchemical Journal
Available online 28 January 2020, 104679
In Press, Journal Pre-proof

Detection of toxicity in some oral antidiabetic drugs using LIBS and LA-TOF-MS

Nasar Ahmad [a, b], Usman Liaqat [c], M. Rafique [b], M. Aslam Baig [a, b], Walid Tawfik [d]

Show more

https://doi.org/10.1016/j.microc.2020.104679

Highlights

- Detection of Carcinogenic elements in the Antidiabetic Tables.
- Rapid and effective method for the identification the of antidiabetic pills without using aggressive chemicals.
- Analytical analysis of German Sugar Cure Core (GSCC), Glucophage and Zolid Plus Antidiabetic tablets.
- Detection of toxicity of unauthorized antidiabetic tablets.
- LIBS complementary with LA-TOF-MS for compositional analysis of pharma-medical tablets.
- Potential of non-destructive techniques for applications in process

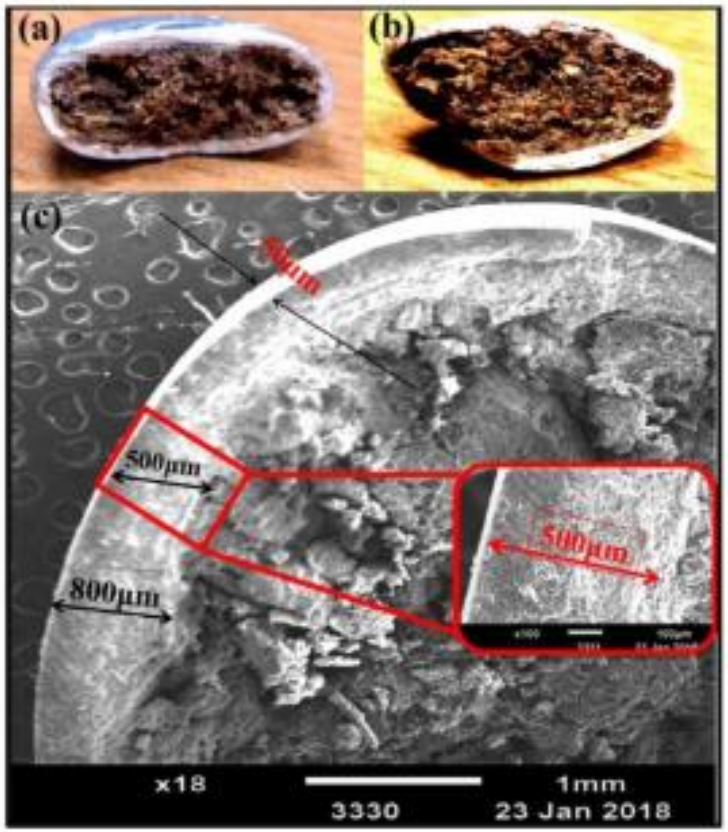
(a)
(b)
(c)
500µm
800µm
500µm
x18
1mm
3330
23 Jan 2018

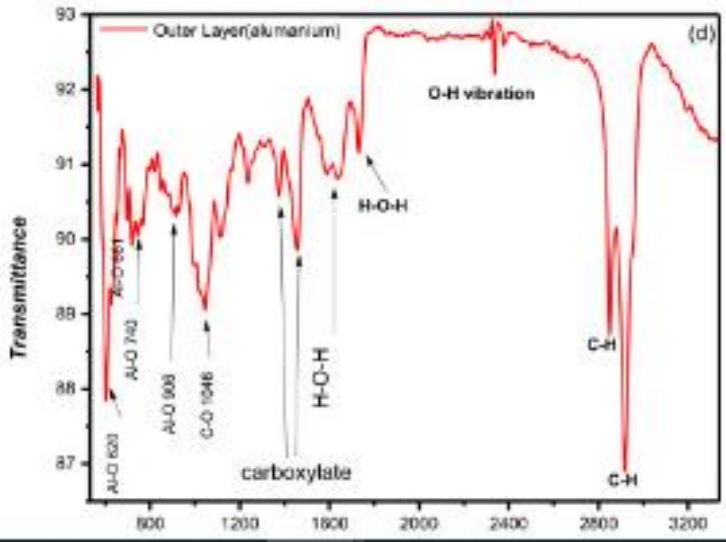
Outer Layer(aluminium)
(d)
Transmittance
O-H vibration
H-O-H
C-H
H-O-H
carboxylate
C-H
Al-O 620
Al-O 740
Al-O 908
C-O 1046
600
1200
1800
2000
2400
2800
3200

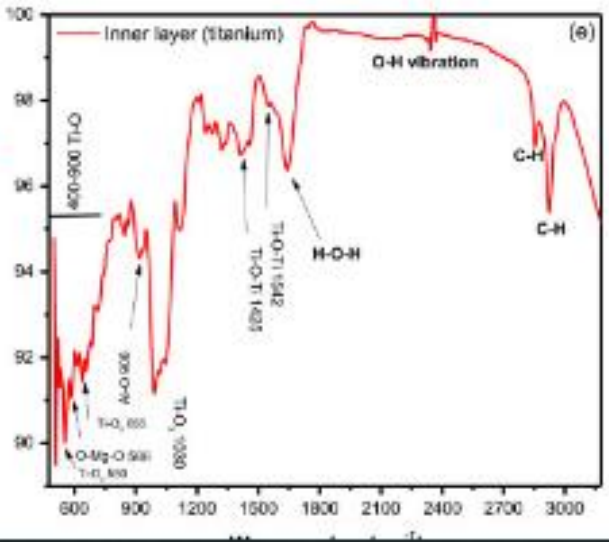
Inner layer (titanium)
(e)
O-H vibration
C-H
C-H
H-O-H
Ti-O-Ti 1542
Ti-O-Ti 1423
400-900 Ti-O
Al-O 908
600
900
1200
1500
1800
2100
2400
2700
3000

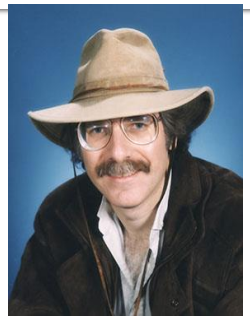

Rick Trebino group at Georgia Institute of Technology, USA

Takayoshi Kobayashi, Tokyo university, Japan

Dong Eon Kim group at POSTECH, south korea

Mostafa el-sayed group at Georgia institute of technology, USA

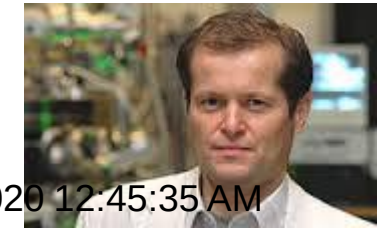

Ferenc Krausz. Max Planck Institute of Quantum Optics, Germany

J P Singh
Visiting Professor from Mississippi State University , USA


Thanks